

# **LONGITUDINAL JOINT DENSITY AND PERMEABILITY IN ASPHALT CONCRETE**

**FINAL REPORT – FHWA-OK-08-07  
ODOT SPR ITEM NUMBER 2197**

by

**Stephen A. Cross, P.E.  
Professor**

and

**Sushanta Bhusal  
Graduate Research Assistant**

**COLLEGE OF ENGINEERING ARCHITECTURE and TECHNOLOGY  
STILLWATER, OKLAHOMA  
OSU: AA-5-17667**

**A Report on Research Sponsored by**

**THE OKLAHOMA DEPARTMENT OF TRANSPORTATION**



**March 2009**

## TECHNICAL REPORT DOCUMENTATION PAGE

1. Report No. FHWA-OK-08-07	2. Government Accession No.	3. Recipient's Catalog No.	
4. Title and Subtitle Longitudinal Joint Density and Permeability in Asphalt Concrete		5. Report Date March 2009	
		6. Performing Organization Code	
7. Authors Stephen A. Cross and Sushanta Bhusal		8. Performing Organization Report No. AA-5-17667	
9. Performing Organization Name and Address Oklahoma State University Civil & Environmental Engineering 207 Engineering South Stillwater, OK 74078		10. Work Unit No.	
		11. Contract or Grant No. Item 2197	
12. Sponsoring Agency Name and Address Oklahoma Department of Transportation Planning & Research Division 200 N.E. 21 <sup>st</sup> Street, Room 3A7 Oklahoma City, OK 73105		13. Type of Report and Period Covered Final Report 11/02/06 – 12/31/08	
		14. Sponsoring Agency Code	
15. Supplementary Notes			
<p>16. Abstract</p> <p>Low longitudinal joint density has been identified as one of the major issues relating to poor asphalt pavement performance. Low longitudinal joint density can lead to premature raveling of the joint and the lower density results in increased permeability of the pavement. Increased permeability allows water to easily enter the pavement resulting in increased susceptibility to moisture induced damage or stripping. The Oklahoma Department of Transportation (ODOT) does not currently have a test method or specification that addresses the problem of low longitudinal joint density. The objective of this study was to obtain the necessary field and laboratory test data to provide information around which a test method and/or specification for control of longitudinal joint density could be written.</p> <p>Three recently constructed pavements were selected for field testing. One pavement was on a county road and the other two pavements were ODOT construction projects. Two or three locations from each project were sampled and tested for a total of seven test sites. Field testing at each site consisted of measuring in-place permeability, measuring pavement density using an electromagnetic device (OHD L-14 Alternate Method B) and obtaining pavement cores at five locations at each test site. Field permeameters used included an NCAT permeameter, a Kentucky air induced permeameter (AIP) and a Romus air permeameter. Laboratory permeability (OHD L-44) was determined on pavement cores.</p> <p>The results from pavement density testing, core density testing, field permeability testing and laboratory permeability testing were analyzed to determine relationships between field permeability, pavement density and laboratory permeability. The suitability of using field permeability at longitudinal joints for control of longitudinal joint density and permeability was evaluated.</p>			
17. Key Words Permeability, Pavement Density, NCAT Permeameter, AIP, Romus Permeameter		18. Distribution Statement No restriction. This publication is available from the office of Planning & Research Division, Oklahoma DOT.	
19. Security Classification. (of this report) Unclassified	20. Security Classification. (of this page) Unclassified	21. No. of Pages 54	22. Price

# SI (METRIC) CONVERSION FACTORS

Approximate Conversions to SI Units					Approximate Conversions from SI Units				
Symbol	When you know	Multiply by	To Find	Symbol	Symbol	When you know	Multiply by	To Find	Symbol
<b>LENGTH</b>					<b>LENGTH</b>				
in	inches	25.40	millimeters	mm	mm	millimeters	0.0394	inches	in
ft	feet	0.3048	meters	m	m	meters	3.281	feet	ft
yd	yards	0.9144	meters	m	m	meters	1.094	yards	yd
mi	miles	1.609	kilometers	km	km	kilometers	0.6214	miles	mi
<b>AREA</b>					<b>AREA</b>				
in <sup>2</sup>	square inches	645.2	square millimeters	mm <sup>2</sup>	mm <sup>2</sup>	square millimeters	0.00155	square inches	in <sup>2</sup>
ft <sup>2</sup>	square feet	0.0929	square meters	m <sup>2</sup>	m <sup>2</sup>	square meters	10.764	square feet	ft <sup>2</sup>
yd <sup>2</sup>	square yards	0.8361	square meters	m <sup>2</sup>	m <sup>2</sup>	square meters	1.196	square yards	yd <sup>2</sup>
ac	acres	0.4047	hectares	ha	ha	hectares	2.471	acres	ac
mi <sup>2</sup>	square miles	2.590	square kilometers	km <sup>2</sup>	km <sup>2</sup>	square kilometers	0.3861	square miles	mi <sup>2</sup>
<b>VOLUME</b>					<b>VOLUME</b>				
fl oz	fluid ounces	29.57	milliliters	mL	mL	milliliters	0.0338	fluid ounces	fl oz
gal	gallons	3.785	liters	L	L	liters	0.2642	gallons	gal
ft <sup>3</sup>	cubic feet	0.0283	cubic meters	m <sup>3</sup>	m <sup>3</sup>	cubic meters	35.315	cubic feet	ft <sup>3</sup>
yd <sup>3</sup>	cubic yards	0.7645	cubic meters	m <sup>3</sup>	m <sup>3</sup>	cubic meters	1.308	cubic yards	yd <sup>3</sup>
<b>MASS</b>					<b>MASS</b>				
oz	ounces	28.35	grams	g	g	grams	0.0353	ounces	oz
lb	pounds	0.4536	kilograms	kg	kg	kilograms	2.205	pounds	lb
T	short tons (2000 lb)	0.907	megagrams	Mg	Mg	megagrams	1.1023	short tons (2000 lb)	T
<b>TEMPERATURE (exact)</b>					<b>TEMPERATURE (exact)</b>				
°F	degrees Fahrenheit	(°F-32)/1.8	degrees Celsius	°C	°C	degrees Celsius	9/5+32	degrees Fahrenheit	°F
<b>FORCE and PRESSURE or STRESS</b>					<b>FORCE and PRESSURE or STRESS</b>				
lbf	poundforce	4.448	Newtons	N	N	Newtons	0.2248	poundforce	lbf
lbf/in <sup>2</sup>	poundforce per square inch	6.895	kilopascals	kPa	kPa	kilopascals	0.1450	poundforce per square inch	lbf/in <sup>2</sup>

The contents of this report reflect the views of the author(s) who is responsible for the facts and accuracy of the data presented herein. The contents do not necessarily reflect the views of the Oklahoma Department of Transportation or the Federal Highway Administration. This report does not constitute a standard, specification or regulation. While trade names may be used in this report, it is not intended as an endorsement of any machine, contractor, process or product.

## TABLE OF CONTENTS

	page
LIST OF FIGURES .....	vii
LIST OF TABLES .....	viii
Chapter 1 INTRODUCTION.....	1
PROBLEM STATEMENT .....	1
OBJECTIVE .....	2
SCOPE .....	2
BENEFITS .....	2
IMPLEMENTATION.....	2
Chapter 2 LITERATURE REVIEW.....	3
PERMEABILITY STUDIES.....	3
LABORATORY PERMEAMETER .....	5
FIELD PERMEAMETERS .....	6
NCAT Field Permeameter .....	6
Kentucky Air Induced Permeameter (AIP).....	8
Romus Air permeameter .....	9
Chapter 3 TEST SITES AND TEST PLAN.....	13
TEST SITES .....	13
TEST PLAN.....	13
Field Sampling and Testing .....	13
Laboratory Testing.....	17
Chapter 4 TEST RESULTS .....	19
MIX PROPERTIES .....	19
Gradation, Asphalt Content and Gmm .....	19
Unit Weight.....	19
FIELD PERMEABILITY .....	19
Chapter 5 ANALYSIS OF DATA .....	26
PERMEABILITY MEASUREMENTS.....	26
Permeability vs. In-Place Voids.....	27
Correlations Between Permeameters .....	30
Summary .....	34
PAVEMENT DENSITY VS. PERMEABILITY .....	34
Percent Compaction .....	34
Difference in Percent Compaction .....	36
Difference in Unit Weight .....	38
<i>Adjacent to Joint Permeability</i> .....	38
<i>Joint Permeability</i> .....	39

	page
Chapter 6 CONCLUSIONS AND RECOMMENDATIONS.....	42
CONCLUSIONS.....	42
RECOMMENDATIONS .....	43
REFERENCES .....	44
APPENDIX A.....	46

## LIST OF FIGURES

	page
Figure 1 OSU’s laboratory permeameters. ....	6
Figure 2 OSU’s NCAT permeameter. ....	7
Figure 3 OSU’s AIP. ....	9
Figure 4 OSU’s Romus air permeameter. ....	11
Figure 5 Romus air permeameter display. ....	12
Figure 6 Permeability and density test locations. ....	14
Figure 7 Electromagnetic gauge used for in-place density testing. ....	14
Figure 8 Measuring field permeability with the Romus air permeameter. ....	15
Figure 9 Measuring field permeability using the AIP. ....	16
Figure 10 Measuring field permeability with NCAT permeameter. ....	16
Figure 11 Obtaining field core for testing. ....	17
Figure 12 OSU’s CoreDry™ apparatus. ....	18
Figure 13 OHD L-44 permeability vs. core voids. ....	28
Figure 14 NCAT permeability vs. core voids. ....	28
Figure 15 AIP permeability vs. core voids. ....	29
Figure 16 Romus permeability vs. core voids. ....	29
Figure 17 Relationship between Kentucky AIP and NCAT permeability. ....	31
Figure 18 Relationship between AIP vacuum pressure and NCAT permeability for Oklahoma mixtures. ....	31
Figure 19 Relationship between NCAT permeability and OHD L-44 permeability. ....	32
Figure 20 Relationship between AIP permeability and OHD L-44 permeability. ....	32
Figure 21 Relationship between Romus permeability and NCAT permeability. ....	33
Figure 22 Relationship between Romus permeability and OHD L-44 permeability. ....	34
Figure 23 Critical void content for laboratory permeability. ....	35
Figure 24 Critical void content for field permeability. ....	35
Figure 25 Difference in core voids vs. OHD L-44 joint permeability. ....	37
Figure 26 Difference in core voids vs. NCAT joint permeability. ....	37
Figure 27 Difference in unit weight vs. change in permeability. ....	39
Figure 28 Critical difference in unit weight for NCAT permeability. ....	40
Figure 29 Relationship between difference in unit weight and OHD L-44 joint permeability. ....	40
Figure 30 Relationship between difference in unit weight and NCAT joint permeability. ....	41

## LIST OF TABLES

	page
Table 1. Critical Permeability and Corresponding Mat Density.....	4
Table 2. Project Locations .....	13
Table 3. Asphalt Content, Gmm and Gradation Analysis, Site 1 .....	21
Table 4. Asphalt Content, Gmm and Gradation Analysis, Site 2 .....	22
Table 5. Asphalt Content, Gmm and Gradation Analysis, Site 3 .....	23
Table 6. Pavement Unit Weight and Air Void Measurements .....	24
Table 7. Field and Laboratory Permeability Results .....	25
Table 8. ANOVA on Permeability Test Results.....	26
Table 9. Results of Duncan’s Analysis on Test Methods .....	27
Table 10. Difference in Mat Properties Across Longitudinal Joint .....	36

# Chapter 1

## INTRODUCTION

### PROBLEM STATEMENT

Low longitudinal joint density has been identified by the National Center for Asphalt Technology (NCAT) as one of the current issues relating to asphalt pavement performance (1). Low density at longitudinal joints has been identified as a major factor in premature deterioration of hot mix asphalt (HMA) pavements. Low longitudinal joint density can lead to premature raveling of the joint and the lower density results in increased permeability of the pavement. The increased permeability allows water to easily enter the pavement resulting in increased susceptibility to moisture induced damage or stripping.

It is generally accepted that one cannot compact a longitudinal joint to the same density as the adjoining mat. A well constructed longitudinal joint should have a density within 2 percent of the mat in the same vicinity (2). There is a large or steep density gradient across the joint and the mat density is significantly higher 6 inches from the joint than it is adjacent to the joint (1).

There are numerous methods and procedures for constructing longitudinal joints. Methods that have been successfully utilized include 3:1 and 12:1 tapered joints with and without notches, edge restraining devices, cutting wheels and rubberized joint adhesives. Workmanship has been identified as a major factor in constructing quality longitudinal joints (3).

Rather than specify a method of longitudinal joint construction, most owner agencies prefer to specify a final product and let the contractor determine the methods and/or equipment. However, due to the steep density gradient that exists at longitudinal joints it is recommended that DOTs spell out exactly where and how to test joint density (1,3).

Pavement cores have traditionally been used to evaluate pavement density or compaction. Nuclear and non nuclear gauges have been utilized as well but both require correlation to densities obtained from cores. The reported drawback to using gauges to measure longitudinal joint density is the inability of the gauge to seat firmly on the joint, making it impossible to get an accurate reading directly at the joint (4). Cores can directly measure joint density; however, density results are not immediately available and patching of the hole is required which can lead to water infiltration.

Field permeameters have recently been developed that can readily measure HMA permeability. If a correlation can be obtained between longitudinal joint density and field permeability then a simple direct method would be available to control longitudinal joint permeability and indirectly control longitudinal joint density.

## **OBJECTIVE**

The Oklahoma Department of Transportation (ODOT) does not currently have a test method or specification that addresses the problem of low longitudinal joint density. The objective of this study was to obtain the necessary field and laboratory test data to provide the information around which a test method and/or specification for control of longitudinal joint density could be written.

## **SCOPE**

Three recently constructed pavements were selected for field testing. One pavement was on a county road and the other two pavements were ODOT construction projects. Two or three locations from each project were sampled and tested for a total of seven test sites. Field testing at each site consisted of measuring in-place permeability, measuring pavement density using an electromagnetic device (OHD L-14 Alternate Method B) and obtaining pavement cores at five locations at each test site. Field permeameters used included an NCAT permeameter, a Kentucky air induced permeameter (AIP) and a Romus air permeameter. Laboratory permeability (OHD L-44) was determined on the pavement cores.

The results from the pavement density testing, core density testing, field permeability testing and laboratory permeability testing were analyzed to determine relationships between field permeability, pavement density and laboratory permeability. The suitability of using field permeability at longitudinal joints for control of longitudinal joint density and permeability was evaluated.

## **BENEFITS**

The development of a test method or specification around field permeability measurements would provide ODOT with an efficient, timely and non destructive method to identify and reduce longitudinal joint permeability and increase longitudinal joint density. Increased longitudinal joint density and reduced permeability would result in increased pavement life and reduced costs to the agency and traveling public.

## **IMPLEMENTATION**

If successful, the proposed research would result in a new test method and or specification for the agency to control longitudinal joint density and permeability.

## **Chapter 2**

### **Literature Review**

#### **PERMEABILITY STUDIES**

The original implementation of Superpave mixes in the late 1990's resulted in DOTs placing coarser mixtures than they had in the past. Almost immediately there were reports of permeability issues with these coarse graded Superpave mixtures. Not only was there concern about permeability of the mixtures but issues concerning longitudinal joint density arose. In 1997 Kandhal and Mallick (2) reported on the field performance of twelve different longitudinal joint construction techniques from 30 different test sections in Michigan, Wisconsin, Colorado and Pennsylvania. The twelve longitudinal joint construction techniques were:

1. Rolling from hot side,
2. Rolling from cold side,
3. Rolling from hot side 6 inches away from joint,
4. 12:1 tapered joint without tack coat,
5. 12:1 tapered joint with tack coat,
6. Edge restraining device,
7. Cutting wheel with tack coat,
8. Cutting wheel without tack coat,
9. Joint maker,
10. 3:1 tapered joint with 1 inch vertical offset,
11. Rubberized asphalt tack coat and
12. New Jersey 3:1 wedge with infrared heating.

The findings from this study (2) were that overall joint density highly influenced performance of the construction techniques with high density indicating better performance. The authors concluded that DOTs should specify minimum compaction levels to be achieved at the longitudinal joint and recommended that density be not more than two percent lower than the density specified in the lanes away from the joint. The 12:1 tapered joint was one of the better performing joint construction methods followed by the cutting wheel and edge restraining device. The authors recommended rolling longitudinal joints from the hot side with a vibratory roller as soon as possible and overlapping the cold side with 1.5 inches of HMA.

In 2002 Kandhal et al. (4) made a follow-up report on his previous study. Kandhal reported that after 6 years, longitudinal joints constructed with rubberized joint material gave the best performance followed by joints made with the cutting wheel. Rolling from the hot side 6 inches away from the joint and the New Jersey 3:1 notched wedge joint performed reasonably well. Kandhal recommended either rubberized joint material or notched wedge joints with rolling from the hot side, preferably 6 inches away from the joint. He further recommended specifying a minimum compaction level at the

longitudinal joint of no more than two percent lower than the mat. Kandhal reported that joint density would have to be determined with cores as it would not be possible to properly seat a nuclear density gauge on the joint.

In 2001 Cooley et al. (5) evaluated coarse graded Superpave mixtures for permeability. It should be noted that ODOT mixes would be classified as fine graded mixes. Cooley et al. reported that strong relationships were observed between field permeability and in-place voids for coarse graded Superpave mixes and that the nominal maximum aggregate size (NMAS) of the mixture greatly influenced permeability of the pavement. Cooley reported in-place densities where mixtures became excessively permeable and selected critical permeability values based on NMAS of the mixture. The values are summarized below.

Table 1. Critical Permeability and Corresponding Mat Density

NMAS	Density Mix Excessively Permeable	Critical Field Permeability ( $10^{-5}$ cm/sec)
9.5 mm	92.3%	100
12.5 mm	92.3%	100
19 mm	94.5%	120
25 mm	95.6%	150

In a follow up study, Cooley et al. (6) evaluated field permeability and laboratory permeability from 23 on-going HMA construction projects. Cooley et al. reported a good relationship between permeability (field and laboratory) and pavement density for coarse graded Superpave mixtures. NMAS was found to have an influence on permeability as well as lift thickness. Larger NMAS and smaller lift thickness resulted in higher permeability. Cooley reported reasonable relationships between field permeability and laboratory permeability indicating that laboratory permeability measurements during mix design had the potential to help control permeability of a mixture.

Mallick et al. (7) performed a follow up study to Cooley's NCAT studies on several pavements and coarse graded mixtures in Maine. Mallick concluded again that air voids have a significant effect on permeability and that NMAS has a significant effect with an order of magnitude increase in permeability at the same void content noted with an increase in NMAS. A decrease in laboratory permeability was noted with an increase in layer thickness.

In 2007 Schmitt et al. (8) reported on the findings from a permeability study in Wisconsin. The purpose of the study was to develop permeability and density acceptance criteria for Wisconsin HMA pavements. Twenty in service pavements, 3 to 11 years in age, were evaluated. The surface mixtures were all fine-graded mixtures.

The researchers (8) concluded that the test pavements were all nearly impermeable with water permeability rates from 0 to  $5 \times 10^{-5}$  cm/sec. Water permeability between the wheel paths was reported as generally higher than in the wheel paths. Air permeability (Romus

device) rates were a factor of 10 greater than water permeability. Air permeability tended downward with an increase in density while water permeability had no discernable trend. No relationship between surface layer thickness and permeability was found and pavement age did not influence permeability. Higher traffic appeared to reduce permeability. Mixtures with higher VMA had higher permeability. The researchers reported it was not possible to establish definitive criteria for permeability and density as they related to pavement performance.

There are numerous other permeability studies available all with similar conclusions. A study by CTC & Associates (9) is a good summary of available DOT sponsored research. Numerous longitudinal joint construction procedures are available that can produce a satisfactory longitudinal joint. The consensus of NAPA and NCAT appears to be let the contractor determine the construction method and the owner/agency specify the required performance. NCAT reports that a well constructed longitudinal joint will have a density approximately two percent less than the adjoining mat (1,2,3).

### **LABORATORY PERMEAMETERS**

Laboratory permeability of HMA samples has typically been performed using a falling head permeameter. At one time there was an ASTM standard test method for determining permeability of HMA samples, *ASTM D 3637 Standard Test Method for Permeability of Bituminous Mixtures*. However, the standard was withdrawn in 1998 and has not been replaced. However, in an attempt to control permeability of HMA pavements, many DOTs specify minimum water permeability of mix design samples as a part of their mix design procedure. ODOT has their own test procedure, OHD L-44 (10). The procedure seems to be very similar to Florida Test Method FM 5-565 and the withdrawn ASTM test method. The procedure is applicable to laboratory compacted samples and field core samples. Recommended heights for field core samples are between 50 mm and 115 mm. It should be noted that some of the recovered layer thickness of the surface mix from the sites sampled in this study were less than 50 mm thick.

OHD L-44 determines the coefficient of permeability of an HMA sample using a falling head permeability test. The equation is shown below [1] (10).

$$k = (aL/At) * \ln (h1/h2) * C \quad [1]$$

where: k = coefficient of permeability, cm/sec  
a = inside cross-sectional area of the graduated cylinder, cm<sup>2</sup>  
L = average thickness of the test specimen, cm  
A = average cross-sectional area of the test specimen, cm<sup>2</sup>  
t = elapsed time between h1 and h2, sec.  
h1 = initial head across the test specimen, cm  
h2 = final head across the test specimen, cm  
C = temperature correction for viscosity of water, a temperature of 68°F (20°C) is used as the standard  
ln = Natural Logarithm

Permeability is reported in units of  $10^{-5}$  cm/sec and measured permeability is corrected to a water temperature of 68°F (20°C). Where possible, all permeabilities in this study were reported in the same units at a water temperature of 68°F (20°C). Figure 1 shows OSU's laboratory permeameters.



Figure 1 OSU's laboratory permeameters.

## **FIELD PERMEAMETERS**

### **NCAT Field Permeameter**

The NCAT field permeameter was developed by NCAT and is commercially available from various vendors. Figure 2 shows OSU's NCAT permeameter. The one used in this study was purchased from Gilson, Inc. The test is a falling head permeability test using water as the permeate. During the test the time required for water in a graduated standpipe to pass through two timing marks is recorded and the permeability calculated using formula [2] (11) shown below. The timing marks must be within one of four different diameter standpipes. The standpipe is selected based on permeability of the pavement with the larger diameter standpipes being used for more permeable mixtures.



Figure 2 OSU's NCAT permeameter.

$$k = (aL/At) * \ln (h1/h2) \quad [2]$$

where: k = coefficient of permeability, cm/sec

a = inside cross-sectional area of standpipe, cm<sup>2</sup>  
 (varies depending on tier used for testing)

Tier 1 = 2.85 cm<sup>2</sup>

Tier 2 = 15.52 cm<sup>2</sup>

Tier 3 = 38.32 cm<sup>2</sup>

Tier 4 = 167.53 cm<sup>2</sup>

L = length of sample (thickness of the asphalt mat), cm

A = cross-sectional area of permeameter through which water can  
 penetrate the pavement, 214 cm<sup>2</sup>

t = elapsed time between h1 and h2, sec.

h1 = initial head, cm

h2 = final head, cm

ln = Natural Logarithm

Testing was performed following the manufacturer's recommendations (11) as no standard test method exists. Permeability is a function of the temperature of the water used as the permeate. During testing, the water temperature was measured and the permeability corrected to 68°F (20°C) by multiplying the calculated permeability from equation [2] by the appropriate correction factor (C) from table 1 of OHD L-44 (10).

There are many reported drawbacks to the NCAT permeameter; however, these drawbacks apply to most field permeameters. Creating a water tight seal is always a problem, especially with coarse surface textured pavement. Plumber's putty was found to work well for forming a water tight seal. The high water head required with relative impermeable pavements can lift the NCAT permeameter; therefore, weights are required to hold the permeameter in place. The large head forces water out through the path of

least resistance and this is not always down or into the pavement as water was often seen exiting the pavement surface a few inches from the permeameter. A final criticism of the NCAT permeameter is determination of flow path or flow length. This is a criticism of all field permeameters. Laboratory permeameters measure flow in one direction, vertical. Field permeameters measure flow in the radial as well as vertical directions making the flow path length a guess. For this study, the same thickness used in OHD L-44, the thickness of the core, was used for calculating field permeabilities.

### **Kentucky Air Induced Permeameter (AIP)**

The AIP was developed by the Kentucky Transportation Center (12) from a comprehensive study of field and laboratory on construction projects in Kentucky. Besides developing the AIP and a standard test method, numerous conclusions on pavement permeability in general were reached. The authors concluded that density had a significant effect on field permeability and that above 92 percent compaction there is a dramatic decrease in field permeability. The 92 percent compaction level was not related to NMAAS of the mixture as in other studies. There was a wide variation in permeability reported across the compacted mat with the highest permeability occurring at the longitudinal joint. Joint permeability was reported as several orders of magnitude larger than at the center of the lane.

The researchers (12) also developed the AIP. The AIP was reported to be highly correlated to the NCAT permeameter. The major advantage of the AIP was listed as reduced test time for pavements with low permeability. There was not a good correlation found between laboratory permeability and either the NCAT permeameter or the AIP.

The procedure for determining permeability of a pavement using the AIP is contained in Kentucky Method 64-449-05 (13). The AIP consists of a LEXAN chamber with ports to connect a Multi-Venturi vacuum cube (Venturi meter) and a vacuum gauge capable of reading from 0 to 700 mm Hg with less than a 0.01 percent error. An air compressor is attached to the venturi meter that delivers a constant air pressure of  $68 \pm 3$  psi. Caulk or plumbers putty is applied to the base of the AIP to form an air tight seal. Vacuum pressure helps to seal the AIP to the pavement surface, weights are not required. A valve is opened on the Venturi meter to allow air flow from the air compressor. This pulls a vacuum inside the AIP and the dial gauge records the minimum air or vacuum pressure. Testing time should not exceed 15 seconds because delamination or humping of the pavement could occur. It is not recommended to perform this test when the pavement temperature exceeds 130°F due to possible delamination. OSU's AIP is shown in figure 3.



Figure 3 OSU's AIP.

According to Kentucky Method 64-449-05 (12), the permeability can be calculated from the following formula:

$$k = 25,757.538 V^{-1.556} \quad [3]$$

where: k = permeability, ft/day and  
V = vacuum reading in mm Hg.

It should be noted that the AIP does not measure permeability; the equation is a correlation to NCAT permeability (12). Therefore, the AIP calculates or measures an equivalent NCAT permeability. For this study permeability was reported in cm/sec. To convert the above equation from ft/day to cm/sec the permeability from equation [3] was multiplied by 0.000352778. Correction to a standard water temperature of 68°F (20°C) was not possible.

The advantages to the AIP are the ease at which the permeameter seals itself to the pavement surface and the relatively quick testing time. It is not necessary to have a supply of water available for testing. However, the procedure requires an air compressor which means either a gasoline operated air compressor or an electrical generator is required. Another drawback to the AIP is the fact that it does not measure permeability; vacuum pressure is correlated to NCAT permeability.

#### **Romus Air Permeameter**

The Romus air permeameter was developed and is manufactured by Romus, Inc. (14). The device was initially evaluated for use by Kanitpong et al. (15). Kanitpong describes

the procedure for using air to determine permeability of dry porous media. A pressure chamber is substituted for the falling water head and the quantity of air flow through the porous media is related to the pressure drop in the air supply. The test is still a falling head permeability test using the basic equation shown below (15).

$$K = (VL\mu)/(ATPa) \cdot \ln(p_1/p_2) \quad [4]$$

where: K = intrinsic or absolute permeability, length squared

L = is length of specimen

$\mu$  = dynamic viscosity of air at test temperature

A = cross-sectional area of sample

T = time for air pressure to drop from p1 to p2

Pa = atmospheric pressure

p1 = air pressure at time t1

p2 = air pressure at time t2

To convert absolute permeability to an equivalent hydraulic conductivity the following equation is used (15):

$$K = k_w * (\mu_w/\rho_w * g) \quad [5]$$

where: K = intrinsic permeability

$k_w$  = hydraulic conductivity or permeability

$\mu_w$  = dynamic viscosity of water

$\rho_w$  = mass density of water

g = acceleration due to gravity

The mass density of water is in slugs and most engineers do not use slugs routinely in their work. However,  $\rho_w * g$  is equal to the unit weight of a material  $\gamma_w$ , so the unit weight of water at the desired test temperature may be substituted into equation [5] for  $\rho_w * g$ .

To calculate permeability using the Romus air permeameter equations [4] and [5] are combined to the following equation:

$$k_w = (VL\mu\gamma_w) / (ATPa\mu_w) \ln(p_1/p_2) \quad [6]$$

where: all terms have been previously described.

For the Romus air permeameter, the volume of the air chamber, V, is 1.00 cubic foot. The device records the time T, in seconds, required for the air pressure in the chamber to drop from p1, 20 inches of water, to p2, 12 inches of water. The cross-sectional area of the Romus air permeameter, A, is 0.1963 feet (6-inch diameter ring). The air temperature is recorded during testing and the corresponding  $\mu$ , dynamic viscosity of air, is entered into equation [6] (15). For our results, the equivalent permeability of water at 68°F (20°C) was desired, therefore, the dynamic viscosity of water ( $\mu_w$ ) and unit weight of water ( $\gamma_w$ ) at

68°F were used,  $2.096 \text{ (lb s/ft}^2) \times 10^{-5}$  and 62.3152 pcf, respectively. A constant value of atmospheric pressure, Pa, of 2116.8 psf was used for all sites.

The test procedure for measuring permeability using the Romus air permeameter is found in the Appendix. The basic procedure consists of placing the device on the pavement and sealing the device by pumping grease from an attached grease gun into the ring at the base of the device. The device is switched on and a vacuum is pulled on the internal air tank. When a vacuum pressure equal to 22 inches of water is reached, a valve at the base of the permeameter is opened and the time required for the air pressure in the chamber to drop from 20 inches of water to 12 inches of water, in seconds, is recorded. Air is pulled from the pavement into the air chamber by vacuum pressure. The air temperature is recorded and the appropriate viscosity of air and time are input into equation [6]. Equation [6] gives the permeability of water at 68°F (20°C) in units of feet per second. The results were converted to cm/sec by multiplying by 30.48. The unit is completely self contained and runs off of battery power. OSU's Romus air permeameter is shown in figure 4. The top of the device, showing the output (time) is shown in figure 5.



Figure 4 OSU's Romus air permeameter.



Figure 5 Romus air permeameter display.

## Chapter 3 Test Sites and Test Plan

The objective of this study was to obtain the necessary field and laboratory test data to provide the information around which a test method and/or specification for control of longitudinal joint density could be written. To meet the objective the following test plan was carried out.

### TEST SITES

Pavements for testing and evaluation were selected by ODOT with input from the Principal Investigator. Newly constructed pavements or pavements under construction were selected to reduce traffic control requirements and to allow verification of the test procedures on new construction. Three pavements were selected for testing, one with suspected poor longitudinal joint density or construction and two with average to above average longitudinal joint density or construction. Three test locations were evaluated on the first test site and two locations were evaluated on the other two test sites. Test site or project locations are shown in table 2.

Table 2. Project Locations

Site	Route	County	Lane
1	Lakeview Road between Jardot & Fairgrounds	Payne	N/A
2	HWY 33	Payne	Westbound
3	US 81	Kingfisher	Southbound

N/A = Not applicable, county road

### TEST PLAN

#### Field Sampling and Testing

Field sampling and testing consisted of obtaining density measurements, field permeability measurements and obtaining pavement cores from five locations at each test site. Test locations were on the longitudinal joint (location C) adjacent and on both sides of the longitudinal joint (locations B & D) and 1-2 feet away from the longitudinal joint in both adjacent lanes (locations A & E). The five test locations for each test site are shown in figure 6.



Figure 6 Permeability and density test locations.

Density measurements can be affected by water; therefore, they were performed first at each location. The density was obtained in accordance with OHD L-14, Alternate Method B. The testing was performed by ODOT personnel. The electromagnetic gauge used is shown in figure 7.



Figure 7 Electromagnetic gauge used for in-place density testing.

Next, field permeability at each location was determined using two air permeameters, the Romus air permeameter and the AIP. The Romus test was performed first because it uses less pressure and does not draw water to the pavement surface as the AIP can. The Romas test was performed in accordance with the manufacturer’s recommendations (14). The only test data required for the Romus test is air temperature and test time. Figure 8 shows the permeability being measured with the Romus air permeameter.

Following Romus testing, field permeability was measured using the AIP in accordance with Kentucky Test Method KM 449-05 (13). For AIP testing, only vacuum pressure is recorded. Figure 9 shows the permeability being measured with the AIP.

Following air permeability testing, the NCAT permeameter test was performed. The test was performed in accordance with the instructions from the manufacturer (11). Field data recorded includes water temperature and time required for the water to flow from the initial head to the final head. After field permeameter testing was completed, a 6-inch diameter core was obtained directly over the spot where the previous testing was performed. Cores were labeled and transported to the Cummins Asphalt Laboratory at OSU. Figure 10 shows permeability being measured with the NCAT permeameter and figure 11 shows a core being obtained over the location where the permeability measurements were made.



Figure 8 Measuring field permeability with the Romus air permeameter.



Figure 9 Measuring field permeability using the AIP.



Figure 10 Measuring field permeability with NCAT permeameter.



Figure 11 Obtaining field core for testing.

### Laboratory Testing

Field core samples were returned to the laboratory where they were cleaned and labeled. Site 1 consisted of a 2-inch surface mix over a chip seal. Two cores were selected and tested intact using OHD L-44 to determine if the permeability could be measured with the chip seal still attached to the core. The chip seal made the cores impermeable; therefore, the chip seal was removed using a water cooled, diamond studded saw blade. Care was taken to completely remove the chip seal while leaving as much of the core intact as possible. At Site 2, core recovery consisted of the surface mix only. At Site 3, core recovery consisted of the surface and binder mix. However, together they were too tall to be tested for laboratory permeability (OHD L-44). Therefore, the cores were separated into their respective layers by sawing with a water cooled, diamond studded saw blade and tested by layer. The analysis was performed on the surface layer only.

After sawing, cores were cleaned and tested for bulk specific gravity in accordance with OHD L-14 Method A. If water absorption exceeded two percent by volume, the bulk specific gravity was determined in accordance with OHD L-45, the CoreLok™ procedure. Rather than using the oven drying procedure of OHD L-14 to determine dry mass, cores were dried to a constant dry mass using the CoreDry™ apparatus in accordance with ASTM D 7227-06. The CoreDry™ is shown in figure 12.



Figure 12 OSU's CoreDry™ apparatus.

After bulk specific gravity testing, laboratory permeability of the surface mix of each core was determined in accordance with OHD L-44. After permeability testing the petroleum jelly was carefully removed from the sides of the samples and the cores were dried to a constant mass in accordance with ASTM D 7227. After vacuum drying, cores A and E were tested for theoretical maximum specific gravity (Gmm) in accordance with AASHTO T 209. The Gmm from core A was used in subsequent voids calculations for locations A and B. The Gmm from core E was used in subsequent voids calculations for locations D and E. The average Gmm from location A and E was used for voids calculations for location C, the longitudinal joint.

After Gmm testing, asphalt content was determined using an NCAT ignition furnace in accordance with OHD L-26 Method A. Gradation of the recovered aggregate was determined in accordance with AASHTO T 30.

## **Chapter 4 Test Results**

### **MIX PROPERTIES**

#### **Gradation, Asphalt Content and Gmm**

Mix properties of gradation, asphalt content and Gmm, determined from cores A and E from each site are shown in tables 3-5, respectively.

#### **Unit Weight**

Measured unit weights, determined from electromagnetic density testing and from bulk specific gravity testing of pavement cores, are shown in table 6. Electromagnetic density tests are not corrected or correlated to core unit weight as recommended in OHD L-14. A quick test method or check was desired for evaluating longitudinal joint permeability and waiting for core test results could delay joint evaluation. Change in unit weight or difference in unit weight is more useful than magnitude of the pavement unit weight. Over the limited range in unit weights, the difference between corrected and uncorrected readings would be insignificant. The first gauge reading and the average of five gauge reading are shown along with the corresponding air voids. The air voids were calculated from corresponding Gmm values shown tables 3-5. The average Gmm from core A and E was used to calculate air voids for core C, the longitudinal joint. The Gmm from core A was used to calculate air voids for core A and B where the Gmm from core E was used for cores D and E.

### **FIELD PERMEABILITY**

Results of the field permeability testing are shown in Table 7. OHD L-44 corrects permeability to a reference temperature of 68°F (20°C) and reports permeability in units of  $10^{-5}$  cm/sec. Therefore, all permeabilities are reported in units of  $10^{-5}$  cm/sec. Romus and NCAT permeabilities are corrected to a reference temperature of 68°F (20°C). The AIP does not actually measure permeability but uses measured vacuum pressure to estimate NCAT permeability based on a correlation equation developed by the Kentucky Transportation Center (12). AIP permeability and vacuum pressure are recorded in table 7. AIP permeability cannot be normalized to a reference temperature.

The Romus air permeameter uses grease exiting the bottom of a metal ring on the base of the permeameter to seal the device to the pavement. When delivered, the grease did not exit all of the holes in the ring, resulting in an incomplete seal to the pavement. The manufacturer was notified and he recommended carefully enlarging one or more of the holes in the ring. Careful inspection indicated that the size of the holes was not the problem but grease was not traveling completely around the ring. It appeared that the sealed device would have to be opened up to fix the problem or the permeameter returned

to the manufacturer. Due to numerous delays with this project, one of which was delivery of the Romus air permeameter, it was decided not to send the air permeameter back to the manufacturer. Instead, plumbers putty was evaluated as a seal for the base ring. The device was evaluated on a parking lot at OSU and a seal was easily established and reasonable test times for the head to drop the required amount were established.

While testing Site 1 very short Romus air permeameter test times, less than 1 second, were recorded for the air pressure to drop the required amount. The permeability of site 1 was expected to be high but could not be calculated in the field, making the accuracy of measured results unavailable in the field. After testing Site 1, the Romus air permeameter was again tested on a different parking lot at OSU and again longer test times were recorded. The device was assumed to be working satisfactorily and used with plumbers putty for the seal for Sites 2 and 3. It should be noted that the surface of the parking lots at OSU were old, made with what appeared to be 3/8 inch NMAAS mixtures, and appeared rather impermeable.

Table 3. Asphalt Content, Gmm and Gradation Analysis, Site 1

Location	1		2		3		ODOT Type B
	A	E	A	E	A	E	
Sieve Size	Percent Passing						
3/4 inch	100	100	100	100	100	100	100
1/2 inch	98	99	98	97	98	97	90-100
3/8 inch	93	95	92	92	89	92	
No. 4	66	67	66	68	63	66	45-70
No. 8	44	45	44	46	43	44	
No. 16	37	38	36	38	36	36	
No. 30	33	35	33	34	32	33	
No. 50	26	26	24	25	24	25	
No. 100	14	13	12	12	12	12	
No. 200	8.6	7.2	7.1	7.3	7.5	7.0	
% AC	N/A	5.7	5.3	5.2	5.3	5.5	4.7-7.5
DP	N/A	1.26	1.34	1.40	1.42	1.27	0.6-1.2
Gmm	2.492	2.527	2.515	2.550	2.532	2.545	

N/A: printer malfunction, data not available

Table 4. Asphalt Content, Gmm and Gradation Analysis, Site 2

Location	4		5		ODOT S-4
	A	E	A	E	
Sieve Size	Percent Passing				
3/4 inch	100	100	100	100	100
1/2 inch	98	98	98	98	90-100
3/8 inch	90	91	89	90	> 90
No. 4	62	62	61	59	
No. 8	36	35	34	34	34-58
No. 16	25	24	24	24	
No. 30	21	20	20	20	
No. 50	16	16	15	15	
No. 100	10	10	9	10	
No. 200	6.9	6.8	6.3	6.9	2-10
% AC	5.9	5.2	5.9	4.8	≥ 4.6
DP	1.18	1.31	1.08	1.42	0.6-1.6
Gmm	2.524	2.532	2.526	2.543	

Table 5. Asphalt Content, Gmm and Gradation Analysis, Site 3

Location	6		7		ODOT S-4
	A	E	A	E	
Sieve Size	Percent Passing				
3/4 inch	100	100	100	100	100
1/2 inch	96	97	97	98	90-100
3/8 inch	93	92	92	91	> 90
No. 4	60	55	58	54	
No. 8	40	34	38	36	34-58
No. 16	29	23	28	27	
No. 30	24	17	22	22	
No. 50	20	13	18	19	
No. 100	14	7	13	13	
No. 200	7.6	6.7	6.3	6.5	2-10
% AC	4.9	5.0	5.0	5.0	≥ 4.6
DP	1.55	1.34	1.27	1.29	0.6-1.6
Gmm	2.514	2.508	2.507	2.504	

Table 6. Pavement Unit Weight and Air Void Measurements

Site	Location	Core	Gauge Results				Core Results	
			Unit Weight (pcf)		VTM (%)		Unit Weight (pcf)	VTM (%)
			First	Average	First	Average		
1	1	A	141.4	141.0	9.1	9.3	146.4	5.8
1	1	B	137.5	136.2	11.6	12.4	139.8	10.1
1	1	C	130.6	130.5	16.6	16.7	134.4	14.2
1	1	D	137.2	135.7	13.0	13.9	141.8	10.0
1	1	E	136.4	136.5	13.5	13.4	143.3	9.1
1	2	A	148.7	148.5	5.2	5.3	149.0	5.0
1	2	B	138.4	140.7	11.8	10.3	142.6	9.1
1	2	C	135.5	139.7	14.3	11.6	138.9	12.1
1	2	D	143.0	141.2	10.1	11.3	144.8	9.0
1	2	E	148.9	149.1	6.4	6.3	146.1	8.2
1	3	A	145.5	145.4	7.9	8.0	146.9	7.0
1	3	B	140.7	141.4	10.9	10.5	149.3	5.5
1	3	C	114.5	122.4	27.7	22.7	135.9	14.2
1	3	D	137.2	139.1	13.6	12.4	144.6	8.9
1	3	E	139.8	139.0	12.0	12.5	145.4	8.5
2	4	A	146.4	143.7	7.7	9.4	149.0	6.1
2	4	B	133.6	130.6	15.2	17.1	138.3	12.2
2	4	C	127.1	128.7	19.3	18.3	133.7	15.1
2	4	D	136.5	132.3	13.4	16.0	140.5	10.8
2	4	E	141.4	140.6	10.9	11.4	141.9	10.6
2	5	A	144.2	143.3	9.1	9.7	146.0	8.0
2	5	B	135.5	131.4	14.2	16.9	140.0	11.4
2	5	C	127.9	133.5	18.8	15.2	131.2	16.7
2	5	D	136.9	136.9	13.1	13.1	141.0	10.5
2	5	E	148.2	145.1	6.6	8.6	143.9	9.3
3	6	A	150.1	146.1	4.3	6.8	146.7	6.5
3	6	B	147.9	139.5	5.7	11.1	142.2	9.3
3	6	C	130.1	141.2	17.0	9.9	131.3	16.2
3	6	D	147.6	142.4	5.7	9.0	147.0	6.1
3	6	E	152.7	149.7	2.4	4.4	147.6	5.7
3	7	A	139.2	142.1	11.1	9.2	142.2	9.1
3	7	B	137.3	134.4	12.2	14.1	134.6	14.0
3	7	C	129.3	134.1	17.3	14.2	129.5	17.1
3	7	D	139.8	140.5	10.5	10.1	142.1	9.1
3	7	E	143.8	145.0	8.0	7.2	143.4	8.3

Table 7. Field and Laboratory Permeability Results

Location	Core	OHD				AIP
		L44	Romus	NCAT	AIP	Pressure
Permeability ( $10^{-5}$ cm/sec)						(mm Hg)
1	A	52.3	871.4	137.2	273.1	183.0
1	B	208.1	1911.7	429.8	*	*
1	C	464.6	4564.1	1487.4	2097.5	50.0
1	D	190.8	2089.8	353.6	929.6	83.5
1	E	6.5	2182.3	277.4	730.4	97.5
2	A	1.3	3462.5	33.5	171.5	248.0
2	B	129.9	2260.0	274.3	806.3	91.5
2	C	418.4	2553.1	387.1	635.8	106.5
2	D	41.0	1238.5	128.0	411.4	141.0
2	E	21.4	547.8	36.6	214.6	214.0
3	A	2.5	568.7	79.2	138.8	283.5
3	B	31.3	1026.9	143.3	283.7	179.0
3	C	344.4	2252.9	673.6	713.2	99.5
3	D	34.6	1609.0	170.7	413.8	140.5
3	E	8.2	1497.3	173.7	424.2	138.0
4	A	11.8	378.0	30.5	77.2	413.0
4	B	422.1	2740.8	966.2	*	*
4	C	1399.5	4399.2	1629.2	*	*
4	D	404.6	4039.0	981.5	*	*
4	E	301.5	2510.5	669.0	76.5	415.5
5	A	120.8	1174.7	163.1	76.8	414.5
5	B	378.2	2605.3	516.6	76.7	415.0
5	C	2598.7	5486.4	2135.1	*	*
5	D	336.1	2783.0	582.2	884.2	86.0
5	E	303.7	1789.4	451.1	304.1	171.5
6	A	26.7	945.3	199.6	259.7	189.5
6	B	273.4	2323.4	486.2	258.6	190.0
6	C	1669.6	4262.2	1525.5	*	*
6	D	24.2	717.4	178.3	112.2	325.0
6	E	20.0	443.5	89.9	*	*
7	A	243.0	2415.0	524.3	112.5	324.5
7	B	826.6	4792.1	2043.7	112.2	325.0
7	C	1960.1	5307.1	2020.8	*	*
7	D	309.8	2145.9	391.7	*	*
7	E	169.1	1123.8	192.0	*	*

\* vacuum gauge malfunction, reading not available

## Chapter 5 Analysis of Data

### PERMEABILITY MEASUREMENT

The objective of this study was to obtain necessary field and laboratory test data to provide information around which a test method and/or specification for control of longitudinal joint density could be written.

Four different permeameters, three field permeameters and one laboratory permeameter, were used to measure permeability of three different surface mixtures. To determine if the permeameters gave statistically similar results, a 2-way analysis of variance (ANOVA) was performed with test method and site as the main effects. The results of the ANOVA are shown in table 8.

Table 8. ANOVA on Permeability Test Results

Source	Degrees Freedom	Sum Squares	Mean Square	F value	Pr > F
Method	3	86237911.6	28745971	37.29	<0.0001
Site	2	5923959	2961980	3.84	0.0242
Interaction	6	4903174	817196	1.06	0.3905
Error	118	90953632.4	770794		
Total	129	188018678			

The ANOVA results indicate a statistically significant difference in test methods, at a confidence limit exceeding 99.9%, and in sites at a confidence limit exceeding 97%. No statistical difference existed between the interaction of test methods and sites. Table 9 shows results from Duncan's Multiple Range Test on test methods. Means with the same letter not significantly different at a confidence limit of 95% ( $\alpha = 0.05$ ). No statistical difference in test methods was found between OHD L-44, the NCAT permeameter or the AIP. The Romus air permeameter produced permeabilities that were statistically different from the other three methods. Removing the Romus test data from the analysis did not change the significance of the other three test methods, they were still statistically similar.

Table 9. Results of Duncan’s Analysis on Test Methods

Grouping	Mean	N	Method
A	2314.8	35	Romus
B	587.5	35	NCAT
B	423.8	25	AIP
B	393.0	35	L-44

### Permeability vs. In-Place Voids

Permeability has been correlated to in-place air voids. To evaluate how well the permeameters correlated to in-place air voids, regression analysis was performed between the permeameters and in-place air voids determined from pavement cores.

The relationship between in-place air voids and OHD L-44 permeability is shown in figure 13. The relationship has a coefficient of determination ( $R^2$ ) of 0.74 and shows that permeability begins to increase when in-place voids exceed 8 percent and increase drastically when in-place voids exceed 10 percent.

The relationship between in-place voids and field permeability measured using the NCAT permeameter is shown in figure 14. The relationship has a coefficient of determination ( $R^2$ ) of 0.81 and shows that permeability begins to increase when in-place voids exceed 8 percent and increase drastically when in-place voids exceed 10 percent.

The relationship between in-place voids and AIP field permeability is shown in figure 15. The best fit relationship was linear with a coefficient of determination ( $R^2$ ) of 0.30, indicating little to no relationship between AIP and in-place voids.

The relationship between in-place voids and field permeability measured using the Romus air permeameter is shown in figure 16. The best fit relationship was linear and has a coefficient of determination ( $R^2$ ) of 0.73, indicating a linear relationship between permeability and in-place voids. However, according to the literature (6,7,8,16), relationships between in-place voids and permeability are not linear but are exponential or use a power function.

OHD L-44 and the NCAT permeameter both showed a relatively good fit with in-place air voids and the relationship had a shape similar to that found in the literature (6,7,8,16). The Romus air permeameter also had a relatively good fit with in-place air voids; however, the relationship was linear and measured permeability was much larger than that measured with any of the other permeameters. The AIP did not correlate well with in-place voids. However, the AIP does not actually measure permeability; it was

correlated to the NCAT permeameter for Kentucky mixtures (12).

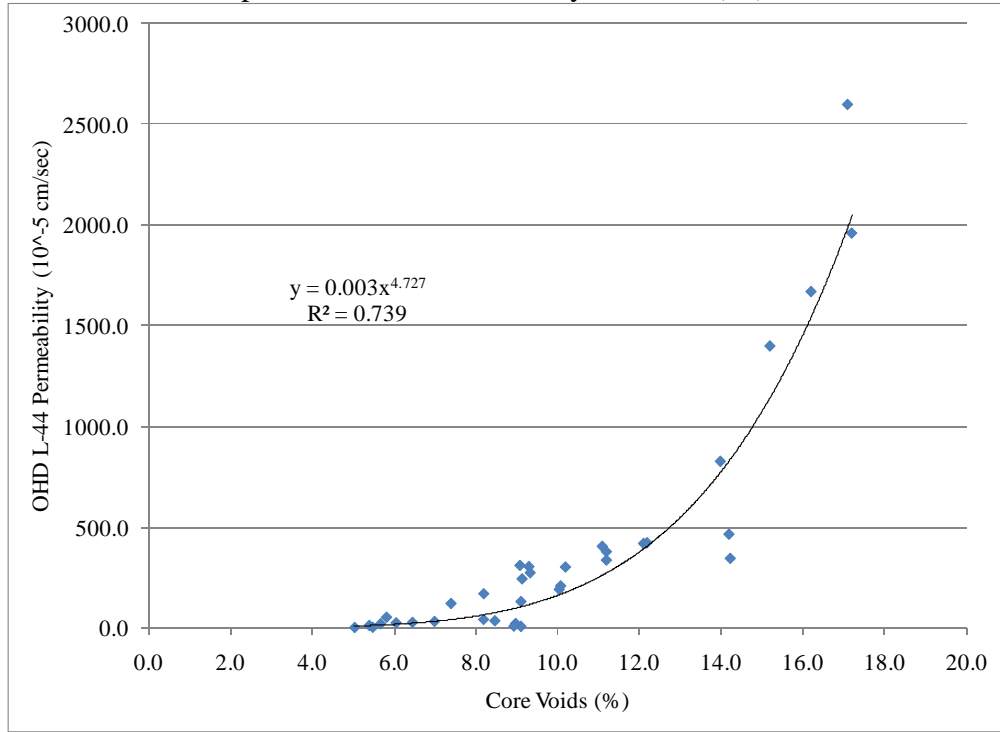


Figure 13 OHD L-44 permeability vs. core voids.

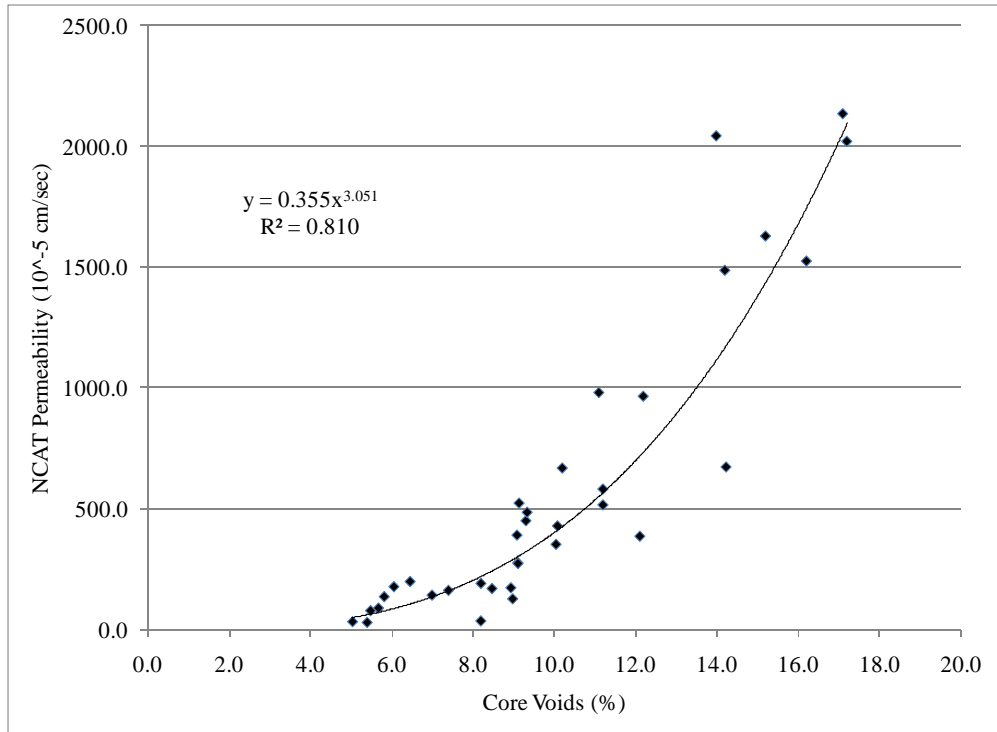


Figure 14 NCAT permeability vs. core voids.

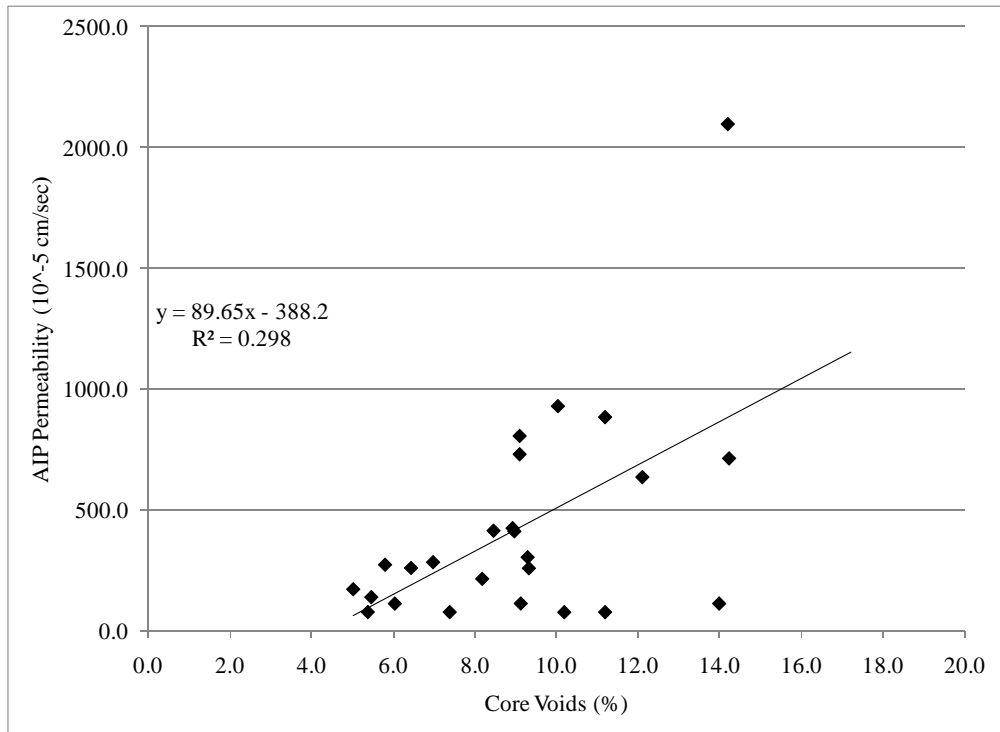


Figure 15 AIP permeability vs. core voids.

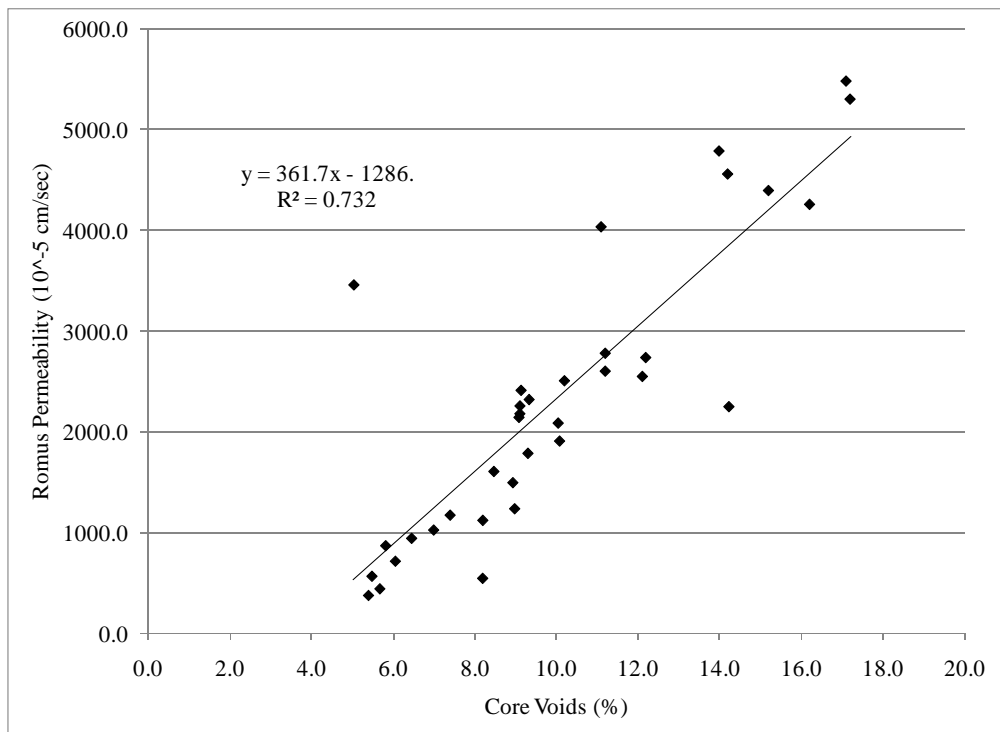


Figure 16 Romus permeability vs. core voids.

## Correlations Between Permeameters

From the means shown in Duncan's analysis (Table 9), there is considerable difference between Romus permeability and the other permeameters. There also appeared to be a difference between the other two field permeameters (NCAT and AIP) and laboratory permeability. OHD L-44 measures vertical permeability where field permeameters allow flow, and therefore measure permeability, in the radial as well as vertical directions. The AIP does not measure permeability; it was correlated to the NCAT permeameter. The relationships between the field and laboratory permeameters are shown in figures 17-22.

The relationship between the Kentucky AIP and the NCAT permeameter is shown in figure 17. The relationship has an  $R^2$  of 0.17, indicating a poor relationship between Kentucky AIP and NCAT permeability for Oklahoma mixtures. AIP permeability is calculated from a formula [3] developed by Kentucky (13). Equation [7] is the Kentucky formula corrected to give permeability in cm/sec rather than feet per day.

$$\text{NCAT permeability (10}^{-5} \text{ cm/sec)} = 9.087 P^{-1.566} \quad [7]$$

Where:  $P$  = vacuum pressure, mmHg

Figure 18 shows the relationship developed between vacuum pressure from the AIP and NCAT permeability for the Oklahoma mixtures evaluated. The relationship is shown in figure 18 and has the same general form as the Kentucky equation shown in equation [7]. The relationship has a goodness of fit ( $R^2$ ) of 0.86. Further evaluation of the equation developed for Oklahoma mixtures was not performed because it is poor technique to evaluate a statistical relationship from the same data set used to establish the relationship. To further evaluate the equation developed for Oklahoma mixtures would require a different data set.

The relationship between NCAT permeability and OHD L-44 permeability is shown in figure 19. The relationship is linear with a goodness of fit ( $R^2$ ) of 0.78. The slope of the best fit line is near 1.00 (0.91), indicating that the difference between OHD L-44 permeability and NCAT field permeability is almost a constant. NCAT field permeability is larger than laboratory permeability by approximately  $230 \times 10^{-5}$  cm/sec. This is as expected due to the differences in flow paths between the two test methods.

The relationship between Kentucky AIP and OHD L-44 permeability is shown in figure 20. The relationship is linear with a goodness of fit ( $R^2$ ) of 0.06 indicating no relationship between the AIP and laboratory permeability.

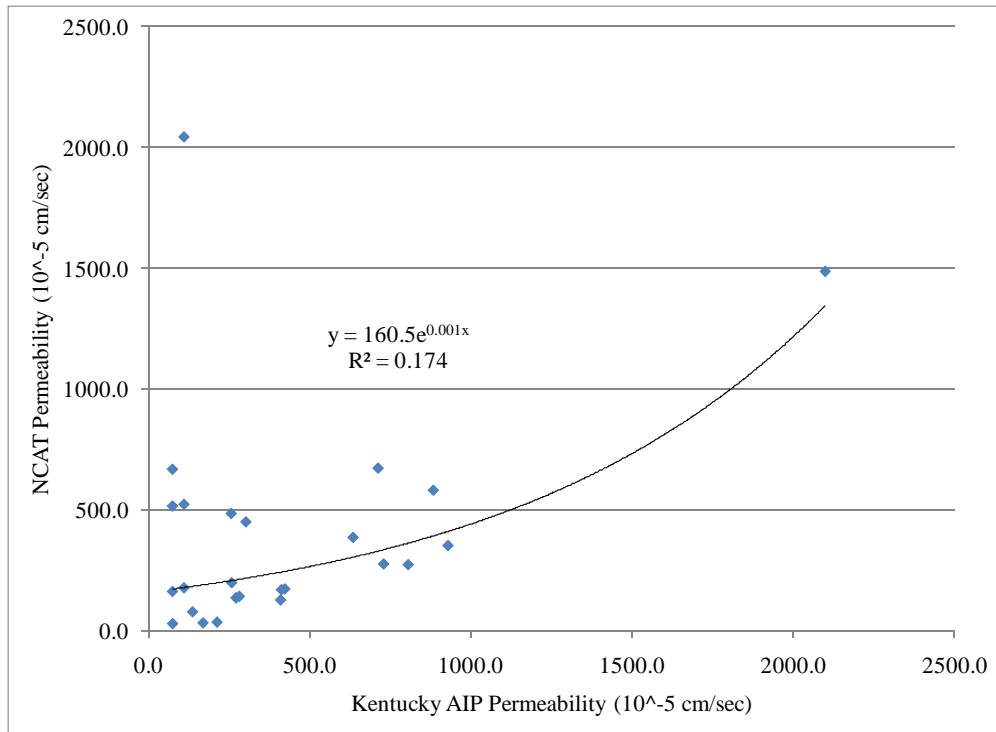


Figure 17 Relationship between Kentucky AIP and NCAT permeability.

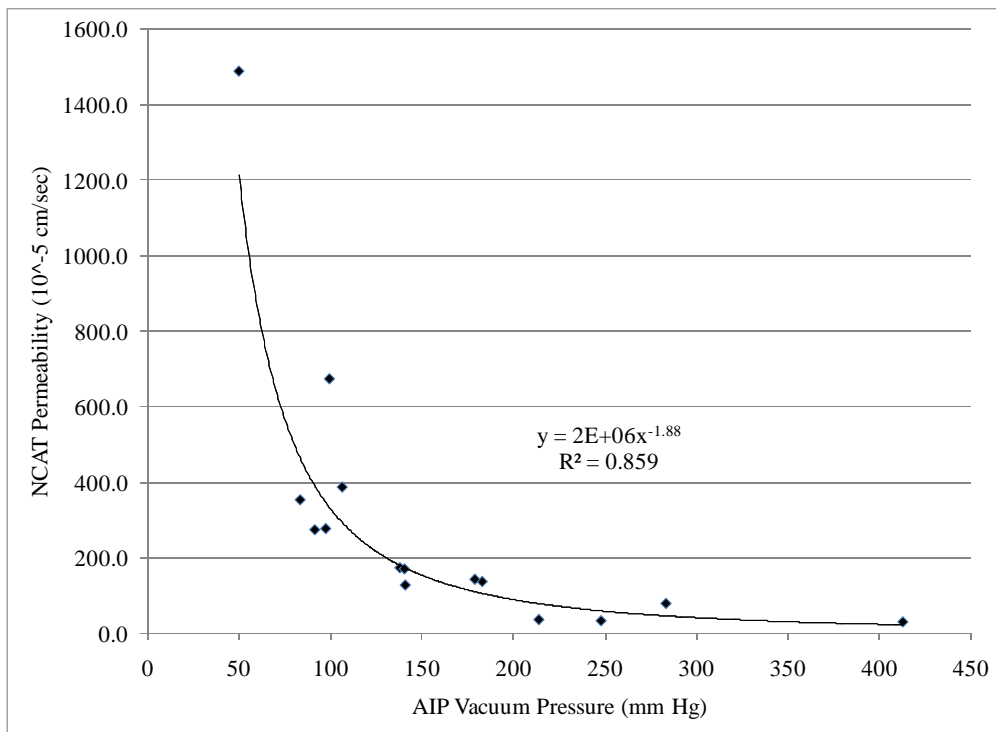


Figure 18. Relationship between AIP vacuum pressure and NCAT permeability for Oklahoma mixtures.

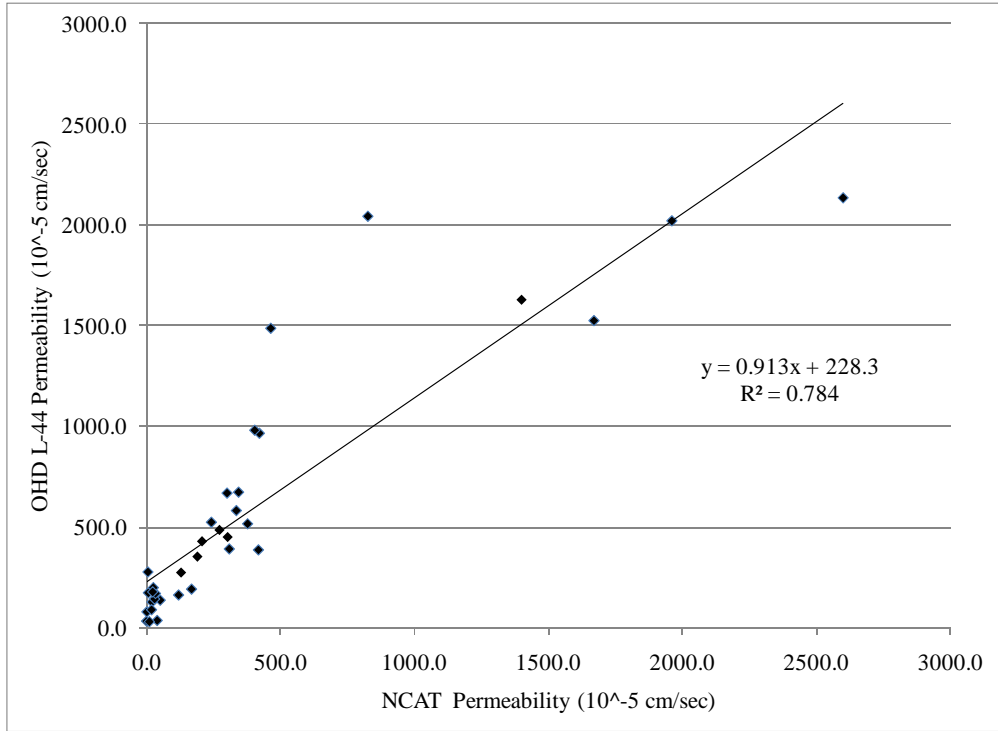
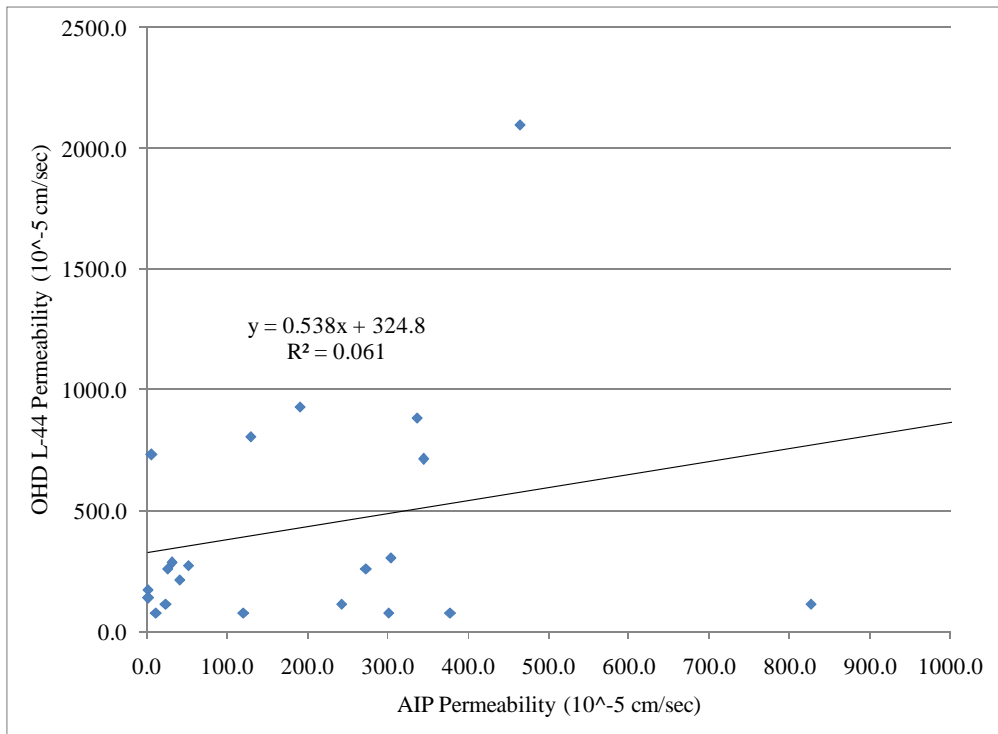


Figure 19 Relationship between NCAT permeability and OHD L-44 permeability.



Although the Romus air permeameter gave considerably larger permeabilities than any of the other permeameters evaluated, there is value in determining if it correlated with either the NCAT permeameter or OHD L-44. The results are shown in figures 21 and 22, respectively. The goodness of fit ( $R^2$ ) was better for the NCAT permeameter ( $R^2 = 0.69$ ) compared to OHD L-44 laboratory permeability ( $R^2 = 0.47$ ). This would be expected as the flow paths for the field permeameters would be similar. The correlation between Romas air permeameter and NCAT permeameter is as strong as the other relationships found. However, due to difficulty in obtaining Romus air permeameter and problems associated with its use in this study, and the fact that correlations with other permeameters were as strong; this researcher does not recommend its use without further evaluation.

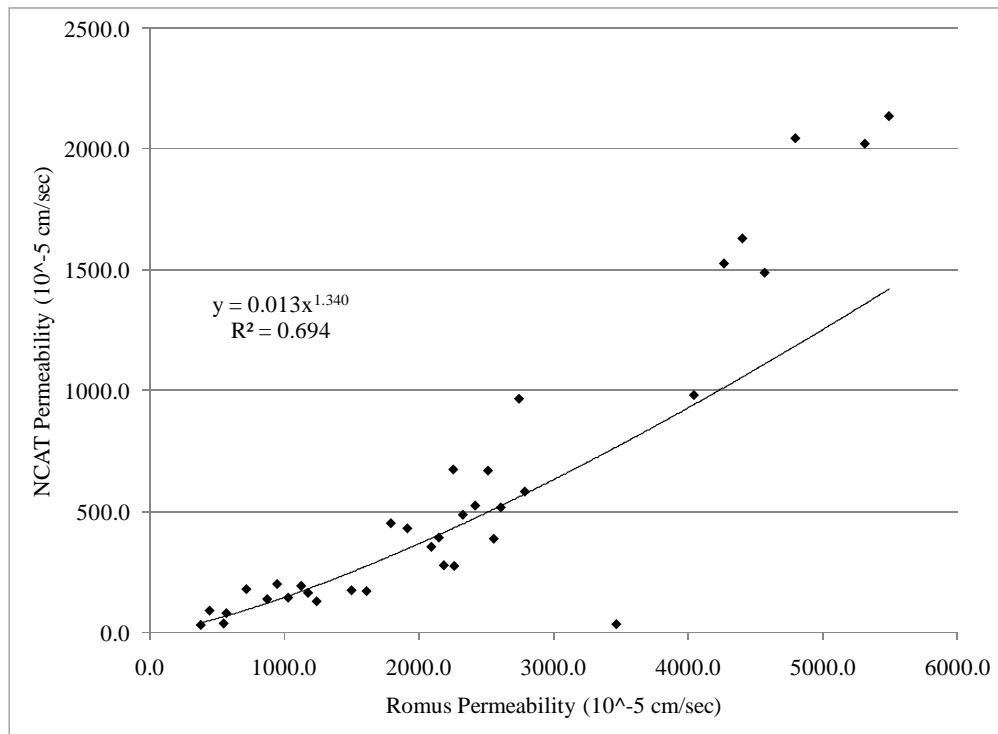


Figure 21 Relationship between Romus permeability and NCAT permeability.

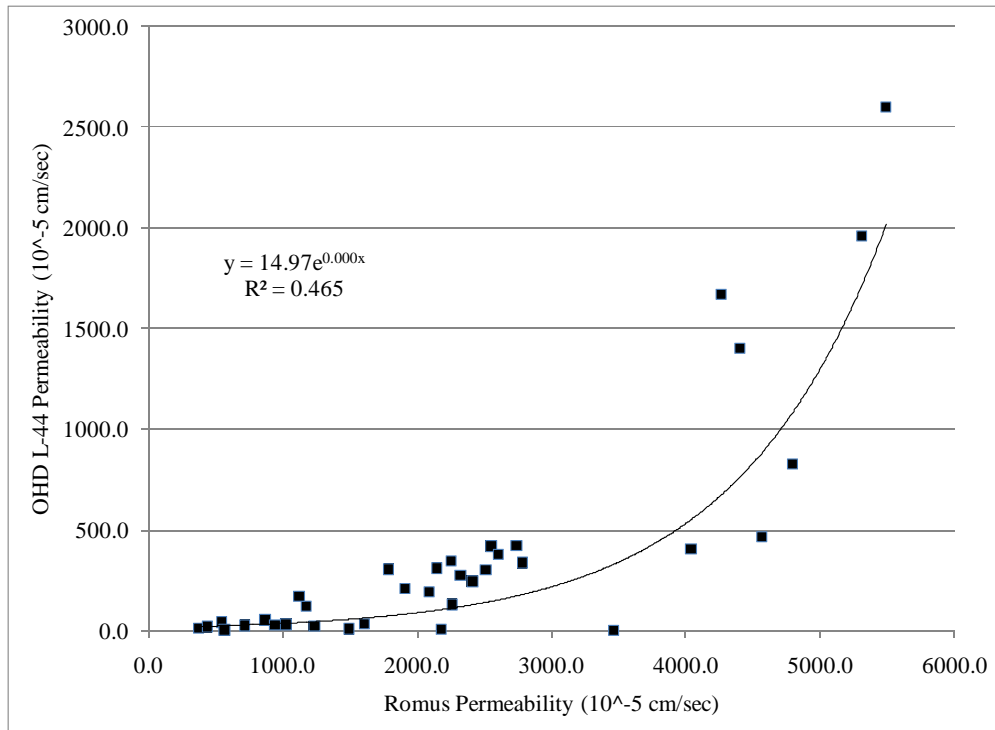


Figure 22 Relationship between Romus permeability and OHD L-44 permeability.

## Summary

Based on the results presented, it is recommended that a specification for longitudinal joint density be developed around either OHD L-44 permeability or the NCAT permeameter. This recommendation is made based on the fact that both NCAT and OHD L-44 permeability correlated well with in-place air voids, as shown in figures 13 and 14, and they correlated well with each other, figure 19.

## PAVEMENT DENSITY VS. PERMEABILITY

### Percent Compaction

Figures 23 and 24 show the relationship between air voids from cores and permeability measured using OHD L-44 and the NCAT permeameter, respectively. ODOT calculates percent compaction based on Gmm; therefore, 100 minus core voids would equal percent compaction. If lines are extended through the straight line portions of the best fit curves for both relationships, critical void contents can be established. As shown in figures 23 and 24, the critical void contents, where permeability shows a marked increase, occurs at approximately 12 and 10 percent voids for OHD L-44 and NCAT permeability, respectively. This corresponds to 88 and 90 percent compaction. For field permeability this critical value of 90 percent compaction agrees with KDOT's (17,18) specification for controlling joint permeability.

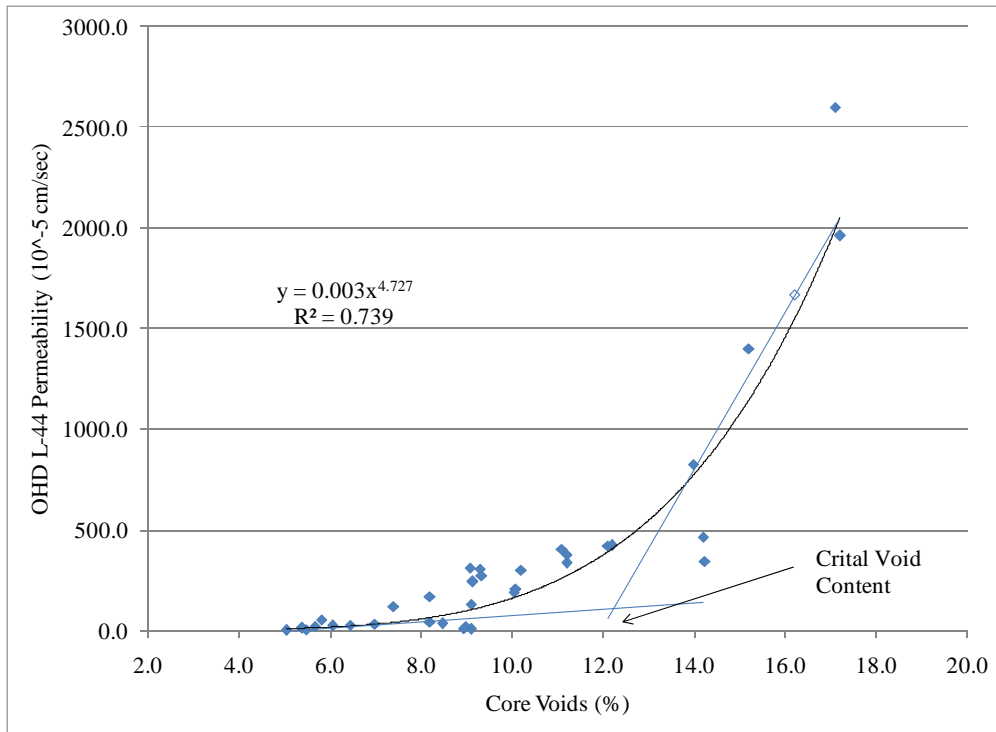


Figure 23 Critical void content for laboratory permeability.

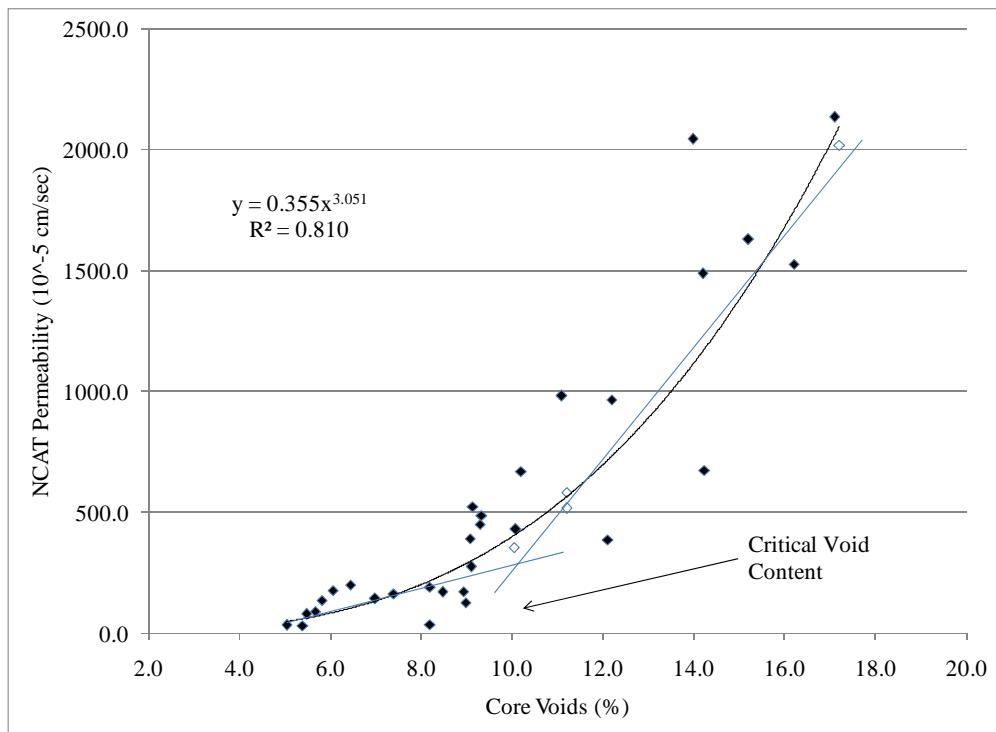


Figure 24 Critical void content for field permeability.

## Difference in Percent Compaction

Many DOTs have proposed controlling longitudinal joint density by controlling the difference in percent compaction between the center of the mat and adjacent to the longitudinal joint. For this study, mat air voids and air voids adjacent to the longitudinal joint would be cores A and B or E and D, respectively. The cold side of the longitudinal joint, mat placed first, is generally expected to have higher voids and higher permeability than the hot side. Therefore, side of the longitudinal joint having the highest air voids and permeability was designated as the cold side of the longitudinal joint. Table 10 shows the difference in air voids between the mat and adjacent to the longitudinal joint for each test location. Permeability at the joint (test location C) and the difference or change in permeability between the mat and adjacent to the longitudinal joint are also shown.

Table 10. Difference in Mat Properties Across Longitudinal Joint

Site	Location	Joint Permeability (10 <sup>-5</sup> cm/sec)		Difference in Core Gauge Voids Unit Wt.		Difference in Permeability (10 <sup>-5</sup> cm/sec)	
		L-44	NCAT	(%)	(pcf)	L-44	NCAT
Cold Side							
1	1	464.6	1487.4	4.3	4.8	155.8	292.6
1	2	418.4	387.1	4.1	7.8	128.6	240.8
1	3	344.4	673.6	1.5	3.9	28.8	64.0
2	4	1399.5	1629.2	6.8	13.1	410.2	935.7
2	5	2598.7	2135.1	3.8	11.9	257.4	353.6
3	6	1669.6	1525.5	2.8	6.6	246.7	286.5
3	7	1960.1	2020.8	4.9	7.7	583.6	1519.4
Hot Side							
1	1	464.6	1487.4	0.9	0.8	184.2	76.2
1	2	418.4	387.1	0.8	7.9	19.6	91.4
1	3	344.4	673.6	0.5	0.0	26.4	3.0
2	4	1399.5	1629.2	0.9	8.2	103.1	312.4
2	5	2598.7	2135.1	1.9	8.2	32.4	131.1
3	6	1669.6	1525.5	0.4	7.3	4.1	88.4
3	7	1960.1	2020.8	0.9	4.5	140.7	199.6

Figures 25 and 26 show the relationship between difference in voids between the mat and adjacent to the longitudinal joint with OHD L-44 and NCAT joint permeability, respectively. The hot and cold sides of the longitudinal joint are indicated on the plots. Relationships between the difference in voids and change in permeability between the mat and adjacent to the longitudinal joint can be seen from figures 13 and 14.

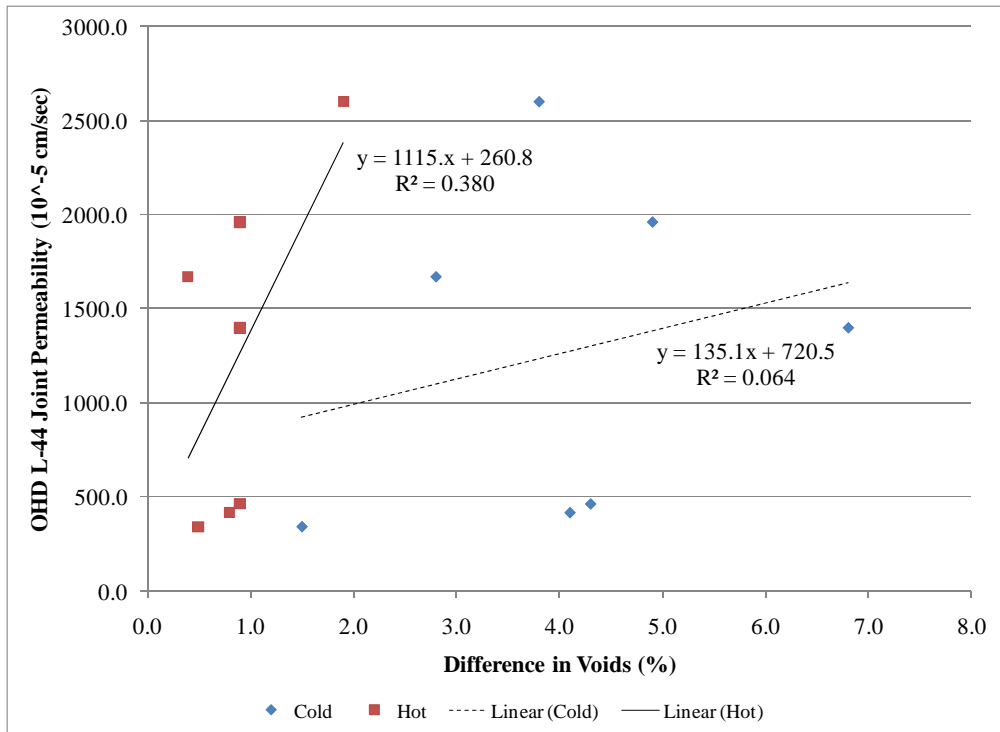


Figure 25 Difference in core voids vs. OHD L-44 joint permeability.

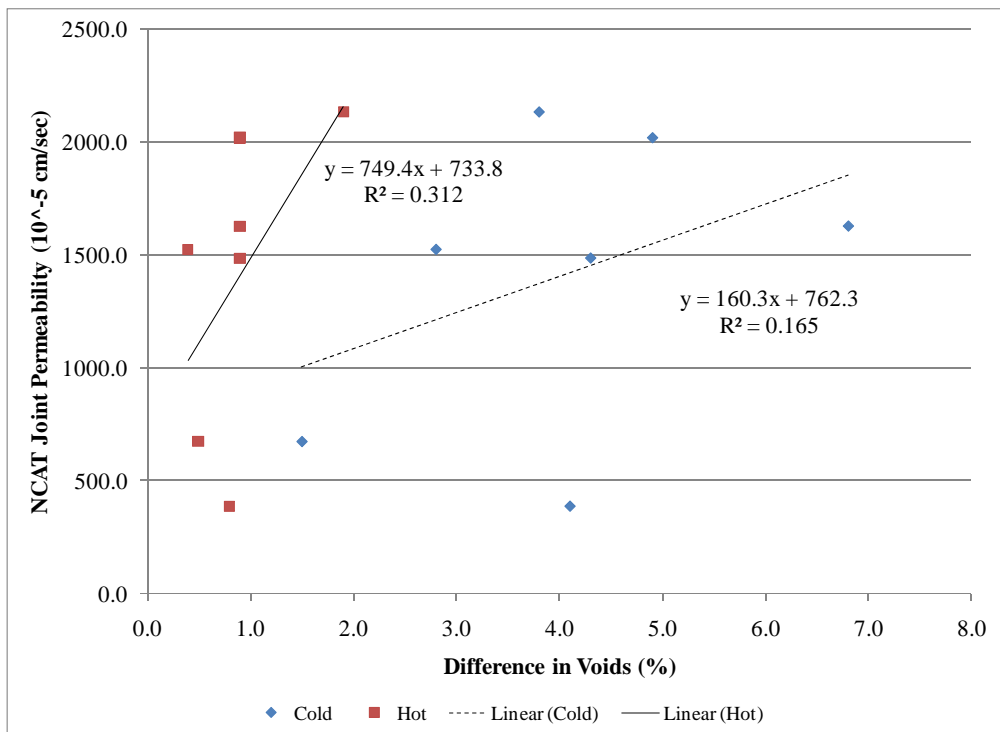


Figure 26 Difference in core voids vs. NCAT joint permeability.

The best fit relationships for the hot and cold sides of the longitudinal joint are shown in each figure. The relationships are poor with  $R^2$  values less than 0.40. The figures do indicate that joint permeability is more related to difference in voids or percent compaction on the hot side of the longitudinal joint rather than the cold side. However, this could be attributed to the small range in difference in air voids for the hot side compared to the cold side.

For laboratory measured joint permeability (figure 25), of the four locations with high joint permeability, OHD L-44 permeability greater than  $500 \times 10^{-5}$  cm/sec, all had a difference in voids for the cold side of greater than 2.5 percent. Of the three locations with OHD L-44 joint permeability less than  $500 \times 10^{-5}$  cm/sec, the difference in voids for the cold side ranged from 1.5 to 4.3 percent. On the hot side, the difference in voids only ranged from 0.4 to 1.9 percent. Of the four locations with high joint permeability, OHD L-44 permeability greater than  $500 \times 10^{-5}$  cm/sec, the difference in voids ranged from 0.4 to 1.9 percent. The three locations with OHD L-44 joint permeability less than  $500 \times 10^{-5}$  cm/sec ranged from 0.5 to 0.9 percent.

For field measured joint permeability (figure 26), of the five locations with high joint permeability, NCAT permeability greater than  $1000 \times 10^{-5}$  cm/sec, all five locations had a difference in voids for the cold side of greater than 2.5 percent. Of the two locations with NCAT joint permeability less than  $500 \times 10^{-5}$  cm/sec, the difference in voids for the cold side were 1.5 and 4.1 percent. Again, on the hot side, the difference in voids ranged from 0.4 to 1.9 percent with the five locations with high permeability ranging from 0.4 to 1.9 percent. The two locations with low NCAT field permeability had a difference in voids of 0.5 and 0.8 percent.

## **Difference in Unit Weight**

### ***Adjacent to Joint Permeability***

As with percent compaction or air voids, many DOTs have proposed controlling longitudinal joint density by controlling difference in unit weight between the mat and adjacent to the longitudinal joint. For this study, mat unit weight and unit weight adjacent to the longitudinal joint would be cores A and B or E and D, respectively. As with voids, the side of the longitudinal joint having the highest air voids and permeability was designated as the cold side of the longitudinal joint. Table 10 shows the difference in unit weight between the mat and adjacent to the longitudinal joint for each test location. Permeability at the joint (test location C) and the difference or change in permeability between the mat and adjacent to the longitudinal joint are also shown.

Figure 27 shows the relationship between difference in unit weight and change in permeability between the mat and adjacent to the longitudinal joint for OHD L-44 and NCAT permeability, respectively. There is no need to differentiate between hot and cold sides of the joint as each side has a specific permeability. No strong relationships were found between difference in unit weight and change in permeability for laboratory

permeability (OHD L-44) but there was a slight relationship ( $R^2$  0.51) for field permeability (NCAT).

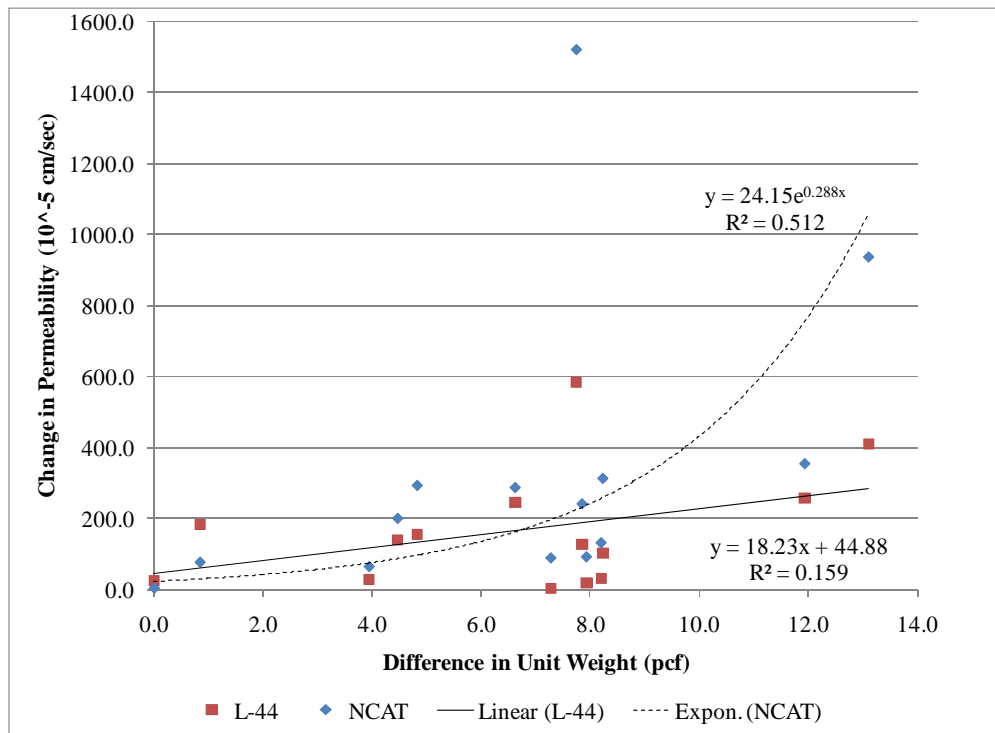


Figure 27 Difference in unit weight vs. change in permeability.

Figure 28 shows the critical difference in unit weight for NCAT permeability. The permeability starts to increase when the difference in unit weight exceeds 5 pcf. The critical difference in unit weight, intersection of straight line portions of the curve, is subjective but appears to be in the 7 to 8 pcf range.

### **Joint Permeability**

Figures 29 and 30 show the relationship between difference in unit weight between the mat and adjacent to the joint for OHD L-44 and NCAT joint permeability, respectively. The hot and cold sides of the joint are indicated on the plots. The relationships are better than with difference in percent compaction or core air voids; however, they are still poor with  $R^2$  values less than 0.45.

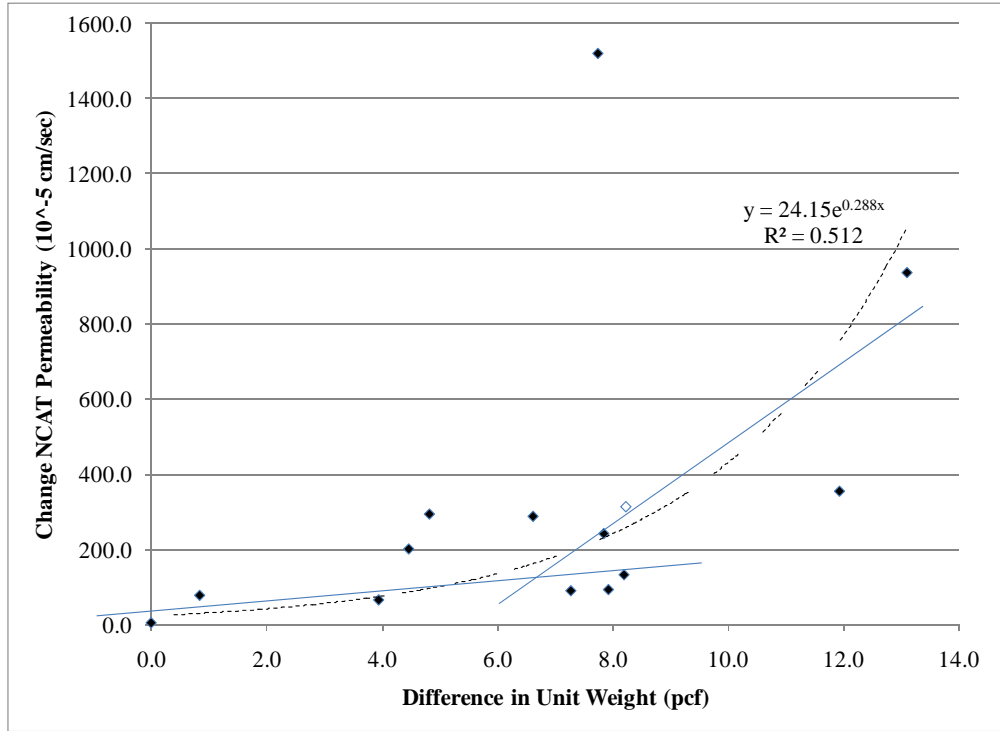


Figure 28 Critical Difference in unit weight for NCAT permeability.

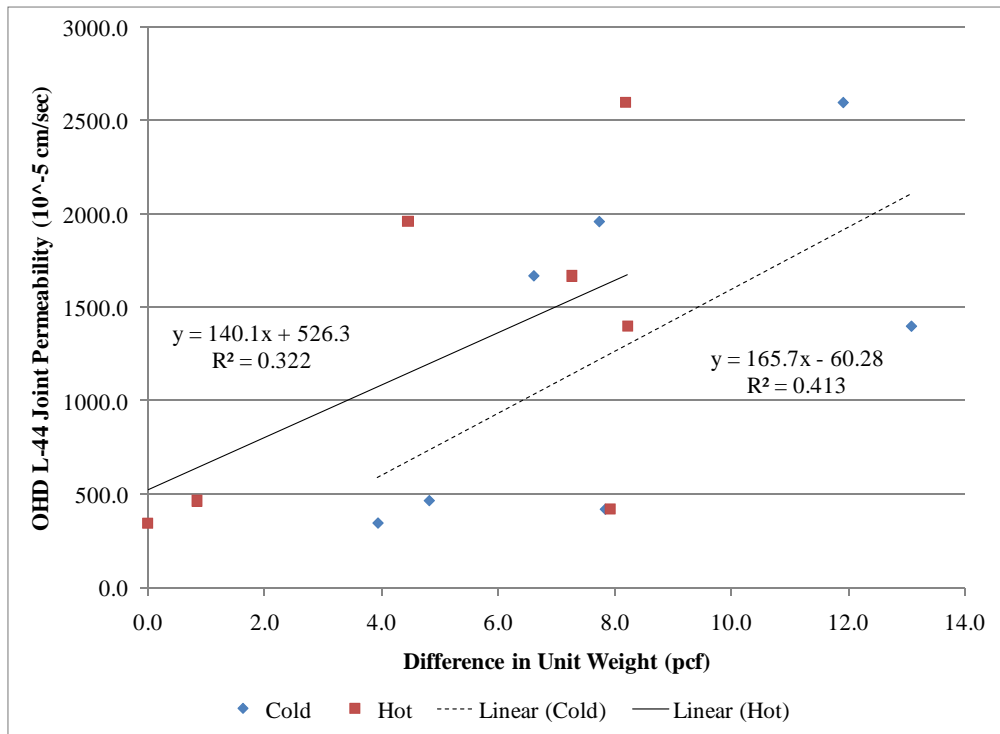


Figure 29 Relationship between difference in unit weight and OHD L-44 joint permeability.

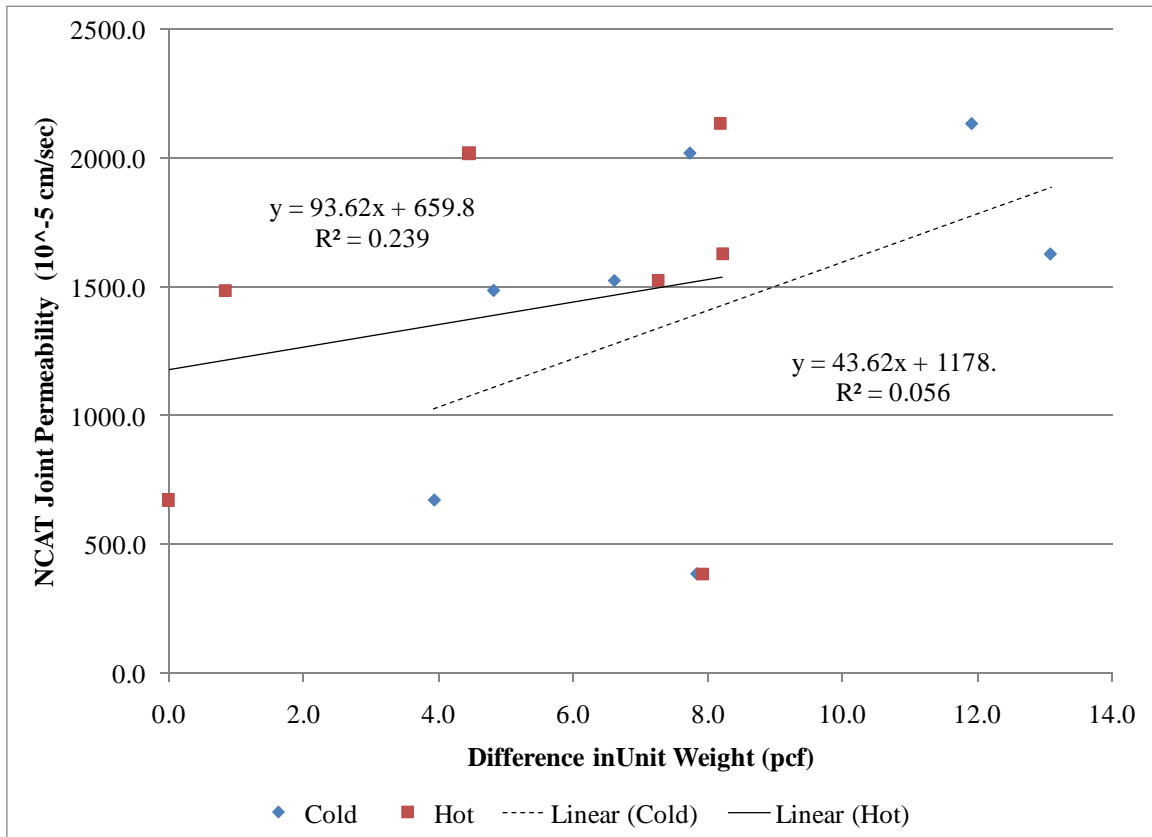


Figure 30 Relationship between difference in unit weight and NCAT joint permeability.

For laboratory measured joint permeability (figure 29), of the four locations with high joint permeability, OHD L-44 permeability greater than  $500 \times 10^{-5}$  cm/sec, all had a difference in unit weight for the cold side of greater than 6.5 pcf. Of the three locations with OHD L-44 joint permeability less than  $500 \times 10^{-5}$  cm/sec, two had a difference in unit weight for the cold side of less than 5.0 pcf. On the hot side, of the four locations with high joint permeability, OHD L-44 permeability greater than  $500 \times 10^{-5}$  cm/sec, all had a difference in unit weight of greater than 4.0 pcf. Of the three locations with OHD L-44 joint permeability less than  $500 \times 10^{-5}$  cm/sec, two had a difference in unit weight of less than 1.0 pcf.

For field measured joint permeability (figure 30), of the five locations with high joint permeability, NCAT permeability greater than  $1000 \times 10^{-5}$  cm/sec, all five had a difference in unit weight for the cold side of greater than 4.5 pcf. Of the two locations with NCAT joint permeability less than  $1000 \times 10^{-5}$  cm/sec, the difference in unit weight for the cold side was 3.9 and 7.8 pcf. On the hot side, of the five locations with high joint permeability, NCAT permeability greater than  $1000 \times 10^{-5}$  cm/sec, four of five locations had a difference in unit weight greater than 4.0 pcf. Of the two locations with NCAT joint permeability less than  $1000 \times 10^{-5}$  cm/sec, the difference in unit weight for the hot side was 0.0 and 7.9 pcf.

## **Chapter 6**

# **CONCLUSIONS AND RECOMMENDATIONS**

### **CONCLUSIONS**

Based on the test results obtained and analysis of test data, the following conclusions are warranted.

1. The Romus air permeameter was the easiest of the three field permeameters to use; however, as delivered the permeameter would not seal to the pavement surface.
2. The AIP tends to seals itself to the pavement surface but requires an air compressor, either a gas powered air compressor or an electric air compressor and generator.
3. The NCAT permeameter is easy to use but requires care to obtain a proper seal.
4. The Romus air permeameter gave the highest permeability, followed by the NCAT permeameter, the AIP and OHD L-44. The statistical analysis indicated no statistically significant difference between the NCAT permeameter, AIP and OHD L-44. The equivalent water permeability at 68°F (20°C) for the Romas air permeameter was an order of magnitude larger than the other three permeameters evaluated.
5. There was a good relationship between in-place voids and permeability measured using OHD L-44, the NCAT permeameter and the Romus air permeameter.
6. There were good correlations between the NCAT permeameter and OHD L-44 and between the NCAT permeameter and the Romus air permeameter.
7. The AIP did not correlate with any of the other permeameters. The AIP does not measure permeability but was correlated to the NCAT permeameter for Kentucky mixtures. A good correlation was found between AIP vacuum pressure and NCAT permeability for Oklahoma mixtures.
8. Permeability starts to increase when in-place voids exceed 8 percent. A critical void content for field and laboratory permeability was found between 10 and 12 percent voids.
9. Joint permeability was more closely related to mix properties on the cold side of the joint rather than the hot side of the joint. The cut-off wheel might be the best method to avoid longitudinal joint permeability issues.
10. There was no good relationship found between difference in core voids (or compaction) from the mat and adjacent to the longitudinal joint and joint permeability.
11. For the cold side of the longitudinal joint, high joint permeability was related to a difference in voids of greater than 2.5 percent.
12. A fair correlation was found between difference in mat density between the mat and adjacent to the longitudinal joint and change in NCAT permeability. A critical difference in mat density was found between 6 and 7 pcf.

13. There were no strong correlations found between the differences in mat density between the mat and adjacent to the longitudinal joint, and joint permeability.
14. For the cold side of the longitudinal joint, a difference in mat density between the mat and adjacent to the joint of greater than 6.5 and 4.5 pcf was related to high OHD L-44 and NCAT joint permeability, respectively.
15. For the hot side of the joint, a difference in mat density between the mat and adjacent to the joint of greater than 4.0 pcf was related to high OHD L-44 and NCAT joint permeability.

## **RECOMMENDATIONS**

There are several ways a specification could be written to help control longitudinal joint density. There were good relationships found between in-place voids (compaction) and permeability and the difference in voids (compaction) and unit weight and permeability. To control permeability and longitudinal joint permeability the following recommendations for consideration as a specification are made.

1. In-place air voids or percent compaction of the mat should not be allowed to drop below 10 percent or 90 percent, respectively.
2. A difference in air voids or percent compaction between the mat and adjacent to the longitudinal joint on the cold side of the mat of greater than 2.5 percent was related to high longitudinal joint permeability.
3. A difference in unit weight between the mat and adjacent to the mat on either side of the longitudinal joint of greater than 4.5 pcf was related to high joint permeability.

## REFERENCES

1. Brown, E. Ray. *Longitudinal Joints – Making Them Last*. Powerpoint Presentation, National Center for Asphalt Technology, Auburn University, Alabama, www.NCAT.org, accessed 2005.
2. Kandhal, Prithvi S. and Rajib B. Mallick. *Longitudinal Joint Construction Techniques for Asphalt Pavements*. NCAT Report 97-4, National Center for Asphalt Technology, Auburn University, Alabama, August 1997.
3. Prowell, Brian D. *Constructing Longitudinal Joints*. Powerpoint Presentation, National Center for Asphalt Technology, Auburn University, Alabama, www.NCAT.org, accessed 2005.
4. Kandhal, Prithvi S., Timothy L. Ramirez and Paul M. Ingram. *Evaluation of Eight Longitudinal Joint Construction Techniques for Asphalt Pavements in Pennsylvania*. NCAT Report 02-03, National Center for Asphalt Technology, Auburn University, Alabama, February 2002.
5. Cooley, L. Allen, E. Ray Brown and Saeed Maghsoodloo. *Development of Critical Field Permeability and Pavement Density Values for Coarse-Graded Superpave Pavements*. NCAT Report 01-03, National Center for Asphalt Technology, Auburn University, Alabama, September 2001.
6. Cooley, L. Allen, Brian D. Prowell and E. Ray Brown. *Issues Pertaining to the Permeability Characteristics of Coarse-Graded Superpave Mixes*. NCAT Report 02-06, National Center for Asphalt Technology, Auburn University, Alabama, July 2002.
7. Mallick, Rajib B., L. Allen Cooley, Matthew R. Teto, Richard L. Bradbury and Dale Peabody. *An Evaluation of Factors Affecting Permeability of Superpave Designed Pavements*. NCAT Report 03-02, National Center for Asphalt Technology, Auburn University, Alabama, June 2003.
8. Schmitt, Robert, Samuel Owusu-Ababio, James Crovetto and Allen L. Cooley. *Development of In-Place Permeability Criteria for HMA Pavement in Wisconsin*, SPR # 0092-06-02, Wisconsin Highway Research Program, Wisconsin DOT, Madison, WI, February 2007.
9. CTC & Associates LLC. *Improved Life for Longitudinal Joints in Asphalt Pavement*. Transportation Synthesis Report, Wisconsin Highway Research Program, Wisconsin DOT, Madison, WI, May 1, 2008.
10. *OHD L-44 Method of Test for Measurement of Water Permeability of Compacted Paving Mixtures*. Materials Division, Oklahoma Department of Transportation, Oklahoma City, OK, September 2007.
11. *Operation & Maintenance Manual, Asphalt Field Permeameter Model AP-1B*. Gilson Company, Inc., Lewis Center, Ohio, August 2004.
12. Allen, L. David, David B. Schultz, Jr. and L. John Fleckenstein. *Development and Proposed Implementation of a Field Permeability Test for Asphalt Concrete*.

- Research Report KTC-01-19/SPR216-00-1F, Kentucky Transportation Center, Lexington, KY, June 2003.
13. *Kentucky Method 64-449-05 Determining the Permeability of In-Place Hot-Mix Asphalt (HMA) Using the Air-Induced Permeameter (AIP)*. Division of Materials, Kentucky Transportation Cabinet, Lexington, KY, December 2004.
  14. *Instructions for the Romus Air Permeameter*. Romus Incorporated, Milwaukee, WI.
  15. Kanitpong, Kunnawee, Hussain Bahia, Jeffrey Russell, Robert Schmitt and James Crovetti. *Effect of Pavement Lift Thickness on Superpave Mix Permeability and Density*. SPR # 0092-02-14c, Wisconsin Highway Research Program, Wisconsin DOT, Madison, WI, April, 2005.
  16. Roberts, Kandhal, Brown, Lee and Kennedy. *Hot Mix Asphalt Materials, Mixture Design and Construction*. NAPA Education Foundation, 2<sup>nd</sup> Edition, Lanham, MD, 1996.
  17. “Joint Density Evaluation Using the Nuclear Density Gauge.” *KDOT Construction Manual, Part V*, Kansas Department of Transportation, Topeka, KS 2007.
  18. KDOT Special Provision 90P-230-R16, Subsection 603.03(e)(2). Kansas Department of Transportation, Topeka, KS 2007.

## APPENDIX A

### INSTRUCTIONS FOR THE ROMUS AIR PERMEAMETER

To power on the air permeameter, press the button. The unit will then run a self-check and will zero the pressure sensor automatically.

To power off the unit, press and hold the button until the “Shut Down” screen is displayed. Then release the button and the unit will power off. Also, the unit will automatically power off after ten minutes have elapsed with no activity.

To take an air permeability reading of an asphalt surface, the following procedure is recommended. Power on the unit. After the self-check is complete, place the unit on the surface being tested and pump the grease handle approximately twenty times. Some experimentation will be needed with this step in the procedure to create an adequate seal. Then, press the button. The valve will open automatically and the system will start recording the elapsed time from when the vacuum pressure reaches twenty inches of water, down to six inches of water. Once the pressure gets below twelve inches of water, the elapsed time will be displayed. If your surface is highly impermeable and the test is taking longer than expected, press the button. You will receive the time and the vacuum pressure at the moment the button was pressed. You may want to repeat the above process to verify that a proper seal was made between the air permeameter and the pavement.

The general operation of the air permeameter is as follows:

-- Power On -Open valve. Zero vacuum sensor  
Turn on vacuum pump At 22 in of H<sub>2</sub>O  
turn vacuum pump off

-- Button Press – Open valve At 20 in of H<sub>2</sub>O  
start timer At 12 in of H<sub>2</sub>O stop timer and display result  
Turn on vacuum pump At 22 in of H<sub>2</sub>O  
turn vacuum pump off

Specifications:

Air tank volume = 1 cuft  
Ring diameter = 6 in  
System voltage = 12v